

Influence of the Pendant Substituent at the C1 Position of a Spirobifluorene Scaffold on the Electronic Properties

Lambert Sicard,^a Clément Brouillac,^a Nicolas Leclerc,^b Sadiara Fall,^c Nicolas Zimmerman,^c Olivier Jeannin,^a Joëlle Rault-Berthelot,^a Cassandre Quinton,^a and Cyril Porié^{a*}

^a Univ Rennes, CNRS, ISCR-UMR 6226, F-35000 Rennes, France

^b Institut de Chimie et Procédés pour l'Énergie, l'Environnement et la Santé (ICPEES), UMR CNRS 7515, 67087 Strasbourg, France.

^c Laboratoire ICube, Université de Strasbourg, UMR CNRS 7357, 67087 Strasbourg, France

TABLE OF CONTENTS

1	General information.....	1
2	Synthesis	3
3	Structural Properties.....	8
4	Electrochemistry	19
5	Copy of NMR spectra.....	29

1 General information

1.1 Synthesis

All manipulations of oxygen and moisture-sensitive materials were conducted with a standard Schlenk technique. All glassware was kept in an oven at 80°C. Argon atmosphere was generated by three repetitive cycles of vacuum/Argon using a Schlenk ramp. Commercially available reagents and solvents were used without further purification other than those detailed below. THF was obtained through a PURE SOLV™ solvent purification system. Light petroleum refers to the fraction with bp 40-60°C. The ultrapure water had a resistivity of 18.2 MΩ cm (Purelab Classic UV) Analytical thin layer chromatography was carried out using aluminum backed plates coated with Merck Kieselgel 60 GF254 and visualized under UV light (at 254 and 360 nm). Flash chromatography was carried out using Teledyne Isco CombiFlash® Rf 400 (UV detection 200-360 nm), over standard silica cartridges (Redisep® Isco or Puriflash® columns Interchim).¹H and ¹³C NMR spectra were recorded using Bruker 300 MHz instruments (¹H frequency, corresponding ¹³C frequency: 75 MHz); chemical shifts were recorded in ppm and J values in Hz. The residual signals for the NMR solvents used are 5.32 ppm (proton) and 54.00 ppm (carbon) for CD₂Cl₂ and XX ppm (proton) and xx ppm (carbon) for CDCl₃.¹ The following abbreviations have been used for the NMR assignment: s for singlet, d for doublet, t for triplet, q for quadruplet and m for multiplet. High resolution mass spectra were recorded at the Centre Régional de Mesures Physiques de l'Ouest (CRMPO-Rennes) on a Thermo Fisher Q-Exactive instrument or a Bruker MaXis 4G or a Bruker Ultraflex III.

Melting point were determined with an Electrothermal® melting point apparatus.

1.2 X-ray

Crystals were picked up with a cryoloop and then frozen at 150 K under a stream of dry N₂. Data were collected on a D8 VENTURE Bruker AXS diffractometer with Mo-K α radiation ($\lambda = 0.71073 \text{ \AA}$).

Structures were solved by direct methods (SIR92)² and refined (SHELXL-2014/7)³ by full-matrix least-squares methods as implemented in the WinGX software package.⁴ An empirical absorption (multi-scan) correction was applied. Hydrogen atoms were introduced at calculated positions (riding model) included in structure factor calculation but not refined. Refinement parameters are summarized in **Erreur ! Source du renvoi introuvable.** and **Erreur ! Source du renvoi introuvable..**

Crystallographic data have been deposited with the Cambridge Crystallographic Data Centre as supplementary publication data: **1-Phen-SBF** (CCDC 2297372), **1-Pyr-SBF** (CCDC 2297373), **1-Napht-SBF** (CCDC 2297374), **1-Anth-SBF** (CCDC 2297377) Copies of the data can be obtained free of charge on application to CCDC, 12 Union Road, Cambridge CB2 1EZ, UK [fax: (+44) 1223-336-033; e-mail: deposit@ccdc.cam.ac.uk].

Figures were generated with Mercury software 3.9.

1.3 Spectroscopic studies

Cyclohexane (spectroscopic grade, Acros), 2-MeTHF (spectroscopic grade, Sigma Aldrich), 1 N solution of sulfuric acid in water (Standard solution, Alfa Aesar), and quinine sulfate dihydrate (99+%, ACROS organics) were used without further purification.

UV-visible spectra were recorded using an UV-Visible spectrophotometer SHIMADZU UV-1605. Molar extinction coefficients (ϵ) were calculated from the gradients extracted from the plots of absorbance vs concentration with five solutions of different concentrations for each sample and at least two mother solutions were prepared.

$$A = \epsilon \times l \times C$$

Above, l refers to the path length and C to the sample concentration.

Emission spectra were recorded with a HORIBA Scientific Fluoromax-4 equipped with a Xenon lamp and a JASCO FP-8300. Triplet energy levels were calculated from the first peak of the phosphorescence spectrum at 77 K. Conversion in electron-volt was obtained with the following formula:

$$E(eV) = \frac{hc}{\lambda}$$

with $h = 6.62607 \times 10^{-34} \text{ J.s}$, $c = 2.99792 \times 10^{17} \text{ nm.s}^{-1}$ and $1 \text{ eV} = 1.60218 \times 10^{-19} \text{ J}$. This equation can be simplified as:

$$E(eV) = \frac{1239.84}{\lambda}$$

with λ formulated in nm.

Quantum yields in solution (ϕ_{sol}) were calculated relative to quinine sulfate ($\phi_{ref} = 0.546$ in H₂SO₄ 1 N). ϕ_{sol} was determined according to the following equation,

$$\phi_{sol} = \phi_{ref} \times \frac{Grad_s}{Grad_r} \times \left(\frac{\eta_s}{\eta_r} \right)^2$$

where subscripts *s* and *r* refer respectively to the sample and reference, *Grad* is the gradient from the plot of integrated fluorescence intensity *vs* absorbance, η is the refracting index of the solvent ($\eta_s = 1.426$ for cyclohexane). Five solutions of different concentration ($A < 0.1$) of the sample and five solutions of the reference (quinine sulfate) were prepared. The integrated area of the fluorescence peak was plotted against the absorbance at the excitation wavelength for both the sample and reference. The gradients of these plots were then injected in the equation to calculate the reported quantum yield value for the sample.

Emission decay measurements were carried out on the HORIBA Scientific Fluoromax-4 equipped with its TCSPC pulsed source interface.

1.4 Electrochemical studies

Electrochemical experiments were performed under argon atmosphere using a Pt disk electrode (diameter 1 mm). The counter electrode was a vitreous carbon rod. The reference electrode was either a silver wire in a 0.1 M AgNO₃ solution in CH₃CN for the studies in oxidation or a silver wire coated by a thin film of AgI (silver(I)iodide) in a 0.1 M Bu₄NI solution in DMF for the studies in reduction. Ferrocene was added to the electrolyte solution at the end of a series of experiments. The ferrocene/ferrocenium (Fc/Fc⁺) couple served as internal standard. The three electrodes cell was connected either to a PAR Model 273 potentiostat/galvanostat (PAR, EG&G, USA) monitored with the ECHEM Software or to a potentiostat/galvanostat (Autolab/PGSTAT101) monitored with the Nova 2.1 Software. Activated Al₂O₃ was added in the electrolytic solution to remove excess moisture. For a further comparison of the electrochemical and optical properties, all potentials are referred to the SCE electrode that was calibrated at - 0.405 V *vs.* Fc/Fc⁺ system. Following the work of Jenekhe,⁵ we estimated the electron affinity (EA) or lowest unoccupied molecular orbital (LUMO) and the ionization potential (IP) or highest occupied molecular orbital (HOMO) from the redox data. The LUMO level was calculated from: LUMO (eV) = -[E_{onset}^{red} (*vs* SCE) + 4.4]. Similarly the HOMO level was calculated from: HOMO (eV) = -[E_{onset}^{ox} (*vs* SCE) + 4.4], based on a SCE energy level of 4.4 eV relative to the vacuum. The electrochemical gap was calculated from: $\Delta E^{el} = |HOMO - LUMO|$ (in eV).

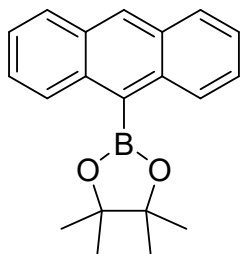
1.5 Theoretical modelling

Full geometry optimization of the ground state and frequency calculation were performed with Density Functional Theory (DFT) using the hybrid Becke-3 0 parameter exchange functional and the Lee-Yang-Parr non-local correlation functional (B3LYP) implemented in the Gaussian 09 (Revision B.01) program suite using the 6-31G(d) basis set and the default convergence criterion implemented in the program. Transition diagrams were obtained through TD-DFT calculations performed using the B3LYP functionals and the 6-311+G(d,p) basis set on the geometry of S0. Geometry optimization of the first excited singlet (S1) and triplet states (T1) was performed using Time-Dependent Density Functional Theory (TD-DFT) calculations using the B3LYP functional and the 6-31+G(d) basis set. Spin density (SD) representation was obtained through TD-DFT calculations performed using the B3LYP functional and the extended 6-311+G(d,p) basis set and a triplet spin on the previously optimized geometry of T1. All stationary points were characterized as minima by analytical frequency calculations. This work was granted access to the HPC resources of CEA-TGCC under the allocation 2022- AD010805032R1 awarded by GENCI. Figures were generated with GaussView 6.0 and GaussSum 3.0 and Mercury software 3.9.

2 Synthesis

2-Iodo-1,1'-biphenyl⁶ and **1-Br-FO**⁷ have been synthesized following previously reported procedures. **2-B(OH)₂-Napht**, **2-B(OH)₂-Phen** and **1-B(OH)₂-Pyr** are commercially available.

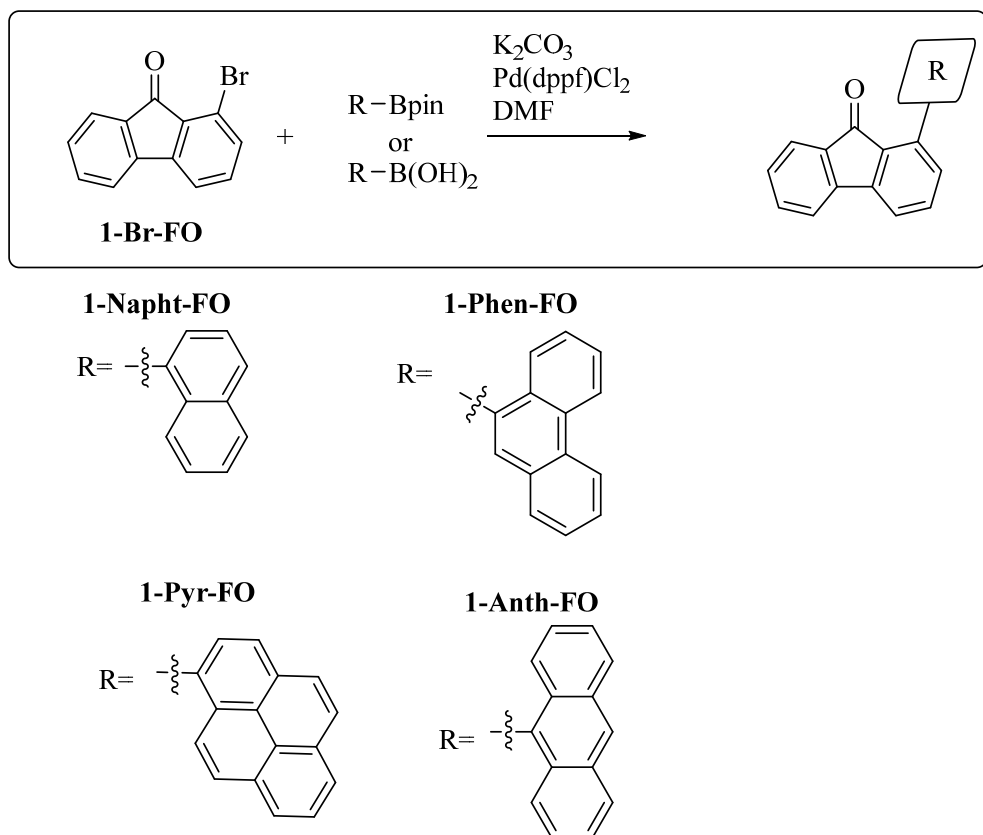
2-(anthracen-9-yl)-4,4,5,5-tetramethyl-1,3,2-dioxaborolane (**2-Bpin-Anth**)



Anhydrous THF (10 mL/mmol) was added to 9-bromoanthracene (1.00 g, 3.89 mmol, 1.0 eq.) under an argon atmosphere and the mixture was cooled down to -78°C. A 2.5 M solution of *n*-BuLi in hexane (1.87 mL, 4.67 mmol, 1.2 eq.) was added dropwise and the solution was stirred at -78°C for 1 h. 2-isopropoxy-4,4,5,5-tetramethyl-1,3,2-dioxaborolane (1.04 mL, 5.25 mmol, 1.35 eq.) was then added all at once. The mixture was allowed to warm up slowly to room temperature and stirred overnight. Diethyl ether (150 mL) was added. The organic layer was washed with water (2 × 100 mL) and brine (100 mL), dried over magnesium sulfate, filtered and concentrated under reduced pressure. After purification by flash chromatography on silica gel [column conditions: silica cartridge (24 g); solid deposit on Celite®; $\lambda_{\text{detection}}$: (254 nm, 280 nm); light petroleum to light petroleum/ Ethyl acetate: 95/5 for 60 min at 35 mL/min], a white powder was obtained (0.995 g, 3.27 mmol); yield 84%; ¹H NMR (300 MHz, CDCl₃) δ 8.54 – 8.43 (m, 3H), 8.00 (dd, *J* = 7.9, 1.9 Hz, 2H), 7.58 – 7.38 (m, 4H), 1.59 (s, 12H). Consistent with previously reported data.⁸

2.1.1 Suzuki coupling general procedure

The 1-bromo-fluorenone derivative **1-Br-FO** (1.0 eq), the corresponding diboron derivative (1.2 eq), potassium carbonate (3.0 eq), and [1,1'-bis(diphenylphosphino)ferrocene]dichloropalladium(II) Pd(dppf)Cl₂·2CH₂Cl₂ (0.05 eq) were dissolved in degassed DMF (15 mL/mmol of **1-Br-FO**) under an argon atmosphere. The mixture was heated to 120°C and stirred overnight. After cooling to room temperature, a saturated solution of ammonium chloride (20-30 mL) was added. The organic layer was extracted with dichloromethane (3 × 50 mL) and washed with brine (2 × 100 mL). The combined organic extracts were dried over magnesium sulfate, filtered, and concentrated under reduced pressure. The residue was purified by flash chromatography on silica gel.



1-Napht-FO

The *title compound* was synthetized according to the Suzuki general procedure using **1-Br-FO** (355 mg, 1.37 mmol), **2-B(OH)₂-Naph** (282 mg, 1.64 mmol), potassium carbonate (568 mg, 4.11 mmol), Pd(dppf)Cl₂.2CH₂Cl₂ (56 mg, 0.07 mmol) in DMF (20 mL). After purification by flash chromatography on silica gel [column conditions: silica cartridge (24 g); solid deposit on Celite®; $\lambda_{\text{detection}}$: (254 nm, 280 nm); dichloromethane/light petroleum (15:85) at 35 mL/min], a yellow powder was obtained (300 mg, 0.98 mmol); yield 71%; mp 203°C; ¹H NMR (300 MHz, CD₂Cl₂) δ 7.96 (ddt, *J* = 8.3, 1.9, 1.0 Hz, 2H), 7.68 – 7.45 (m, 9H), 7.39 (ddd, *J* = 8.3, 6.8, 1.4 Hz, 1H), 7.33 – 7.26 (m, 2H). ¹³C NMR (75 MHz, CDCl₃) δ 192.57, 145.07, 143.78, 140.02, 136.03, 134.45, 134.24, 133.98, 133.44, 132.42, 131.75, 131.60, 129.21, 128.39, 128.36, 126.43, 125.99, 125.74, 125.50, 125.12, 124.17, 120.16, 119.57. HRMS calculated for C₂₇H₁₇O: 357.12739, found: 357.1276 [M+H]⁺

1-Phen-FO

The *title compound* was synthetized according to the Suzuki general procedure using **1-Br-FO** (355 mg, 1.37 mmol), **2-B(OH)₂-Phen** (364 mg, 1.64 mmol), potassium carbonate (568 mg, 4.11 mmol), Pd(dppf)Cl₂.2CH₂Cl₂ (56 mg, 0.07 mmol) in DMF (20 mL). After purification by flash chromatography on silica gel [column conditions: silica cartridge (24 g); solid deposit on Celite®; $\lambda_{\text{detection}}$: (254 nm, 280 nm); dichloromethane/light petroleum (15:85) at 35 mL/min],

a yellow powder was obtained (382 mg, 1.07 mmol); yield 78%; mp 195°C; ¹H NMR (300 MHz, CD₂Cl₂) δ 8.82 (t, *J* = 9.5 Hz, 2H), 8.08 – 7.12 (m, 14H). ¹³C NMR (75 MHz, CDCl₃) δ 192.53, 145.04, 143.83, 139.92, 135.06, 134.48, 134.23, 132.37, 131.91, 131.47, 131.10, 130.49, 130.28, 129.24, 128.85, 127.01, 126.77, 126.73, 126.49, 126.47, 126.30, 124.22, 123.02, 122.71, 120.23, 119.74. HRMS calculated for C₂₇H₁₆O: 356.1196, found: 356.1198 [M]⁺.

1-Anth-FO

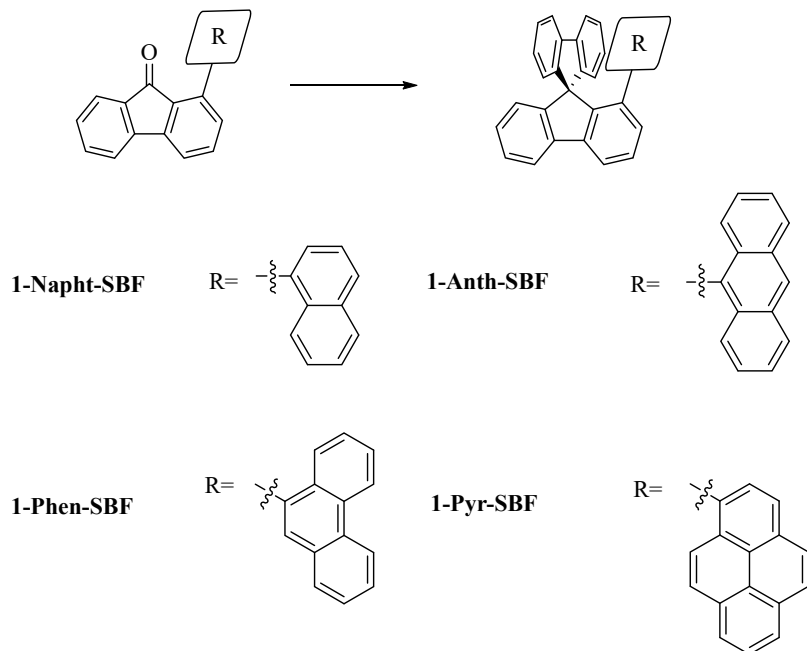
The *title compound* was synthetized according to the Suzuki general procedure using **1-Br-FO** (355 mg, 1.37 mmol), **2-Bpin-Anth** (500 mg, 1.64 mmol), potassium carbonate (138.2 mg, 4.11 mmol), Pd(dppf)Cl₂.2CH₂Cl₂ (56 mg, 0.07 mmol) in DMF (20 mL). After purification by flash chromatography on silica gel [column conditions: silica cartridge (24 g); solid deposit on Celite®; λ_{detection}: (254 nm, 280 nm); dichloromethane/light petroleum (15:85) at 35 mL/min], a yellow powder was obtained (278 mg, 0.78 mmol); yield 55%; mp 236°C; ¹H NMR (300 MHz, CD₂Cl₂) δ 8.58 (s, 1H), 8.10 (d, *J* = 8.5 Hz, 2H), 7.79 – 7.42 (m, 9H), 7.37 – 7.25 (m, 4H). ¹³C NMR (75 MHz, CDCl₃) δ 192.20, 145.23, 143.87, 138.22, 134.46, 134.25, 134.19, 133.27, 132.92, 132.78, 131.32, 129.84, 129.24, 128.65, 127.15, 125.92, 125.53, 125.04, 124.20, 120.27, 119.88. HRMS calculated for C₂₇H₁₇O: 357.1274, found: 357.1276 [M+H]⁺

1-Pyr-FO

The *title compound* was synthetized according to the Suzuki general procedure using **1-Br-FO** (355 mg, 1.37 mmol), **2-B(OH)₂-Pyr** (403 mg, 1.64 mmol), potassium carbonate (568 mg, 4.11 mmol), Pd(dppf)Cl₂.2CH₂Cl₂ (56 mg, 0.07 mmol) in DMF (20 mL). After purification by flash chromatography on silica gel [column conditions: silica cartridge (24 g); solid deposit on Celite®; λ_{detection}: (254 nm, 280 nm); dichloromethane/light petroleum (30:70) at 35 mL/min], an orange powder was obtained (0.247 g, 0.65 mmol); yield 47%; mp 220°C; ¹H NMR (300 MHz, CDCl₃) δ 8.38 – 8.07 (m, 5H), 8.06 – 7.97 (m, 3H), 7.91 (d, *J* = 9.2 Hz, 1H), 7.72 – 7.60 (m, 3H), 7.58 – 7.49 (m, 2H), 7.39 (dd, *J* = 7.4, 1.3 Hz, 1H), 7.33 – 7.25 (m, 1H). ¹³C NMR (75 MHz, CDCl₃) δ 192.63, 145.22, 143.79, 140.49, 134.49, 134.25, 133.96, 133.34, 132.97, 131.63, 131.44, 131.22, 130.99, 129.24, 128.90, 127.57, 127.54, 127.09, 125.89, 125.21, 125.04, 124.95, 124.73, 124.33, 124.21, 120.20, 119.61. HRMS calculated for C₂₉H₁₇O: 381.1274, found: 381.127 [M+H]⁺

2.1.2 1-aryl SBF synthesis general procedure

2-Iodo-1,1'-biphenyl (1.4 eq) was dissolved in dry THF (8.8 mL/mmol) and cooled down to -78°C. A 2.5 M hexane solution of *n*-BuLi (1.5 eq) was then added dropwise to the solution at -78°C. The resulting mixture was stirred at the same temperature for one hour and the corresponding 1-fluorenone-SBF (1 eq) dissolved in dry THF (12 mL/mmol) was added dropwise. The reaction mixture was allowed to warm up to room temperature and stirred overnight. Absolute ethanol (2 mL) was added and the reaction mixture was concentrated under reduced pressure. The residue was dissolved in acetic acid (30 mL/mmol of fluorenone) and the solution was heated to 100°C before 37% hydrochloric acid (1-2 mL) was added dropwise. The resulting mixture was heated under reflux for 4-10 h. The reaction mixture was then cooled down to room temperature and water (20 mL) was added. The organic phase was extracted with dichloromethane (3 × 50 mL) and washed with a saturated aqueous solution of sodium thiosulfate (50 mL), water (2 × 50 mL) and brine (100 mL). The organic layer was then dried over magnesium sulfate, filtrated and concentrated under reduced pressure. The residue was purified by flash chromatography on silica gel.



1-Napht-SBF

The *title compound* was synthetized according to the 1-aryl SBF general procedure using 2-iodo-1,1'-biphenyl (320 mg, 1.14 mmol) in THF (15 mL), *n*-Buli in hexane 2.5 M (0.49 mL, 1.22 mmol), **1-Napht-FO** (250 mg 0.82 mmol) in THF (7 mL), acetic acid (30 mL) and chlorydric acid (1 mL). After purification by flash chromatography on silica gel [column conditions: silica cartridge (24 g); solid deposit on Celite®; $\lambda_{\text{detection}}$: (254 nm, 280 nm); light petroleum at 35 mL/min, a colourless powder was obtained (252 mg, 0.57 mmol); yield 70 %; ^1H NMR (300 MHz, CD₂Cl₂) δ 8.06 – 7.89 (m, 2H), 7.60 – 7.49 (m, 2H), 7.47 – 7.33 (m, 3H), 7.29 (m, 1H), 7.23 – 6.89 (m, 7H), 6.84 – 6.68 (m, 2H), 6.65 – 6.41 (m, 4H), 6.03 (dd, J = 7.0, 1.3 Hz, 1H). ^{13}C NMR (75 MHz, CD₂Cl₂) δ 149.33, 146.39, 145.70, 142.71, 142.20, 141.47, 141.14, 138.09, 135.48, 132.61, 131.43, 130.26, 127.84, 127.59, 127.27, 127.19, 127.00, 126.53, 126.45, 126.11, 124.70, 123.97, 123.49, 123.41, 120.06, 119.26, 118.66, 65.85. ; HRMS calculated for C₃₅H₂₂: 442.1716, found: 442.1719 [M]⁺.

1-Phen-SBF

The *title compound* was synthetized according to the 1-aryl SBF general procedure using 2-iodo-1,1'-biphenyl (275 mg, 0.98 mmol) in THF (15 mL), *n*-Buli in hexane 2.5 M (0.42 mL, 1.05 mmol), **1-Phen-FO** (250 mg 0.70 mmol) in THF, acetic acid (30 mL) and chlorydric acid (1 mL). After purification by flash chromatography on silica gel [column conditions: silica cartridge (24 g); solid deposit on Celite®; $\lambda_{\text{detection}}$: (254 nm, 280 nm); dichloromethane/light petroleum: 5/95 at 35 mL/min, a colourless powder was obtained (281 mg, 0.57 mmol); yield 82 %; ^1H NMR (300 MHz, CD₂Cl₂) δ 8.49 (ddt, J = 8.9, 1.3, 0.7 Hz, 1H), 8.41 (ddt, J = 8.4, 1.2, 0.6 Hz, 1H), 8.06 – 7.94 (m, 2H), 7.62 – 7.52 (m, 2H), 7.48 – 7.33 (m, 3H), 7.21 – 6.96 (m, 8H), 6.88 – 6.79 (m, 1H), 6.62 (ddd, J = 7.6, 1.3, 0.8 Hz, 1H), 6.55 – 6.37 (m, 4H), 6.31 (s, 1H). ^{13}C NMR (75 MHz, CD₂Cl₂) δ 149.79, 149.29, 146.20, 145.29, 142.86, 141.95, 141.45, 141.31, 137.91, 133.63, 130.84, 130.71, 130.34, 129.60, 129.36, 129.26, 127.86, 127.72, 127.66, 127.60, 127.46, 127.20, 126.98, 126.86, 126.54, 126.03, 125.70, 125.44, 123.56, 123.49, 123.25, 121.71, 120.09, 120.03, 119.35, 118.47, 65.91. HRMS calculated for C₃₉H₂₄: 492.1873, found: 492.1877 [M]⁺.

1-Anth-SBF

The *title compound* was synthetized according to the 1-aryl SBF general procedure using 2-iodo-1,1'-biphenyl (220 mg, 0.79 mmol) in THF, *n*-Buli in hexane 2.5M (0.34 mL, 0.84 mmol), **1-Anth-FO** (200 mg 0.56 mmol) in THF, acetic acid (30 mL) and chlorydric acid (1 mL). After purification by flash chromatography on silica gel [column conditions: silica cartridge (24 g); solid deposit on Celite®; $\lambda_{\text{detection}}$: (254 nm, 280 nm); light petroleum at 35 mL/min, a colourless powder was obtained (192 mg, 0.39 mmol); yield 70%; ^1H NMR (300 MHz, CD_2Cl_2) δ 8.15 – 8.09 (m, 2H), 8.00 (dt, J = 7.5, 0.9 Hz, 1H), 7.74 – 7.61 (m, 3H), 7.40 (td, J = 7.5, 1.1 Hz, 1H), 7.18 – 7.10 (m, 3H), 7.05 (td, J = 7.5, 1.2 Hz, 1H), 6.91 – 6.81 (m, 4H), 6.74 – 6.63 (m, 4H), 6.62 – 6.48 (m, 4H), 6.40 (dt, J = 7.6, 0.9 Hz, 1H). ^{13}C NMR (75 MHz, CD_2Cl_2) δ 149.74, 146.58, 145.92, 142.81, 141.50, 140.93, 136.26, 132.48, 130.81, 130.34, 129.43, 128.02, 127.85, 127.55, 127.30, 127.13, 126.71, 126.67, 126.29, 124.18, 124.13, 123.47, 123.34, 120.00, 119.72, 118.42, 66.04. HRMS calculated for $\text{C}_{39}\text{H}_{24}$: 492.1873, found: 492.1876 $[\text{M}]^+$.

1-Pyr-SBF

The *title compound* was synthetized according to the 1-aryl SBF general procedure using 2-iodo-1,1'-biphenyl (424 mg 1.51 mmol) in THF (5 mL), *n*-Buli in hexane 2.5M (0.60 mL, 1.51 mmol), **1-Pyr-FO** (500 mg 1.31 mmol) in THF, acetic acid (30 mL) and chlorydric acid (1 mL). After purification by flash chromatography on silica gel [column conditions: silica cartridge (24 g); solid deposit on Celite®; $\lambda_{\text{detection}}$: (254 nm, 280 nm); light petroleum at 35 mL/min, a colourless powder was obtained (417 mg, 0.80 mmol); yield 61 %; ^1H NMR (300 MHz, CD_2Cl_2) δ 8.33 – 8.11 (m, 8H), 8.06 – 7.89 (m, 6H), 7.72 – 7.63 (m, 4H), 7.57 – 7.50 (m, 3H), 7.41 – 7.38 (m, 1H), 7.33 – 7.27 (m, 2H). ^{13}C NMR (75 MHz, CD_2Cl_2) δ 149.33, 148.70, 146.72, 145.85, 142.71, 142.10, 141.49, 140.93, 138.58, 133.60, 130.99, 130.68, 130.38, 129.80, 128.50, 127.89, 127.71, 127.62, 127.39, 127.27, 127.14, 127.08, 126.90, 126.72, 126.13, 126.02, 125.59, 125.43, 124.45, 124.43, 124.14, 123.68, 123.54, 123.49, 123.40, 122.82, 120.14, 119.85, 119.46, 118.23, 65.91. HRMS calculated for $\text{C}_{41}\text{H}_{24}$: x, 516.18725 found: 516.1879 $[\text{M}]^+$.

3 Structural Properties

X-Ray studies

The centroid to centroid distance, $\text{d}_{\text{C-C}}$, is the distance between two ring centroids (for example Phenyl 1 and Phenyl 2 in the following figure or cyclopentadiene and phenyl in other molecules). θ , the ring slippage angle, is defined as the angle between the normal projection of one ring centroid on the other ring and the centroid / centroid vector (see below). The vertical displacements d_1 or d_2 are defined as the distance between the centroid of one ring and the normal projection of the centroid of the other ring.

For each phenyl ring or cyclopentadienyl ring, $\text{d}_{\text{C-C}}$ and H_1 and H_2 are measured on the X-ray structures allowing to calculate θ_1 and θ_2 .

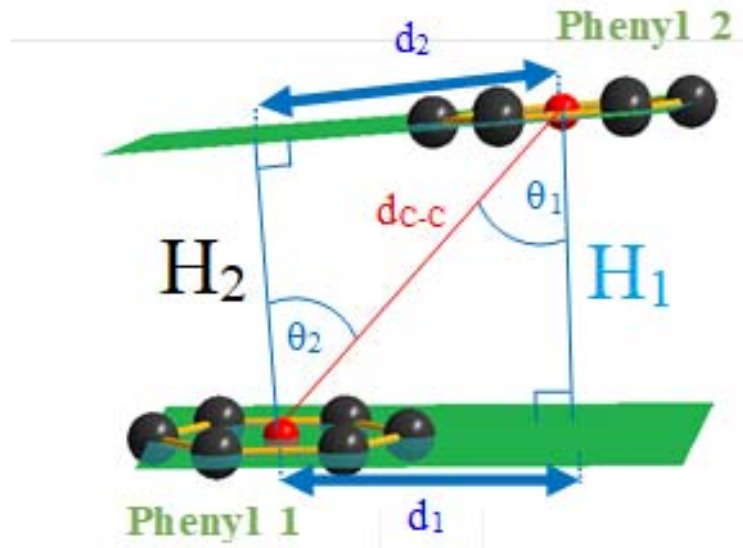
$$\cos \theta_1 = \text{Centroid to plane distance (\AA)} / \text{centroid to centroid distance (\AA)} = \text{H}_1 / \text{d}_{\text{C-C}}$$

$$\cos \theta_2 = \text{Centroid to plane distance (\AA)} / \text{centroid to centroid distance (\AA)} = \text{H}_2 / \text{d}_{\text{C-C}}$$

Then, the vertical displacement d_1 or d_2 are calculated using respectively the following formula:

$$\sin \theta_1 = \text{Vertical displacement (\AA)} / \text{centroid to centroid distance (\AA)} = \text{d}_1 / \text{d}_{\text{C-C}}.$$

$\text{Sin } \theta_2 = \text{Vertical displacement (\AA)} / \text{centroid to centroid distance (\AA)} = \mathbf{d}_2 / \mathbf{d}_{\text{C-C}}$.



1-Naph-SBF

$d_{\text{C-C}}$: 3.899 Å between 2 Phenyl units

H_1 : 3.549 Å

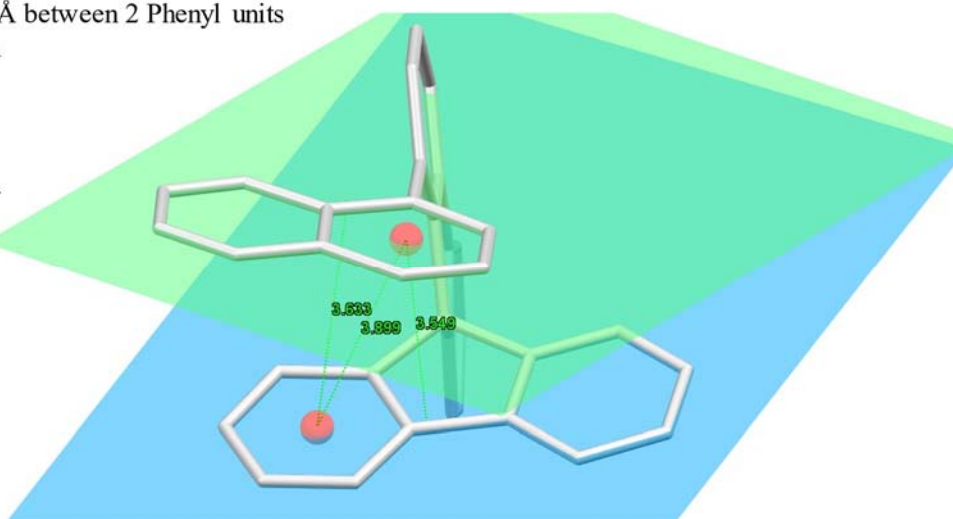
d_1 : 1.61 Å

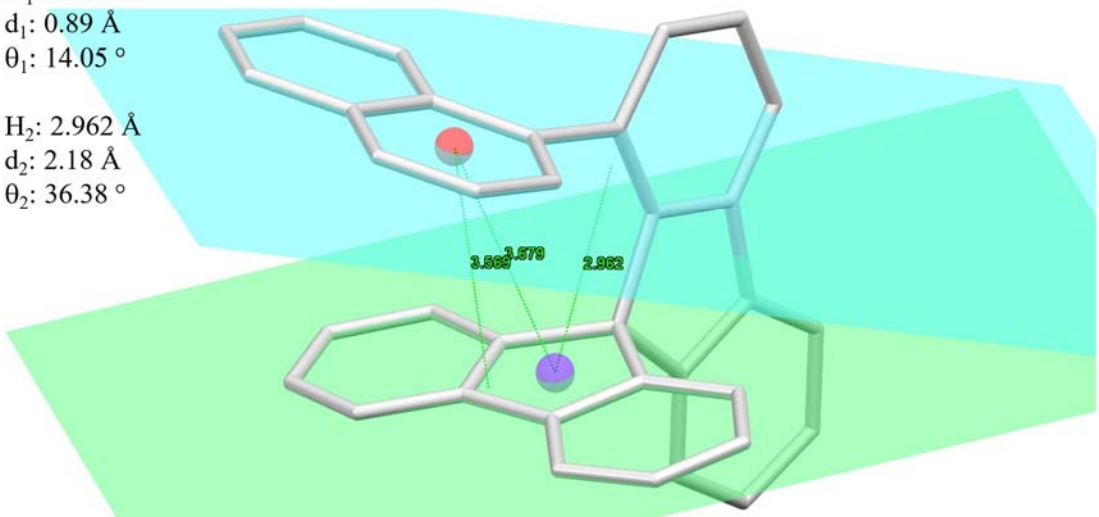
θ_1 : 24.4 °

H_2 : 3.633 Å

d_2 : 1.41 Å

θ_2 : 21.21 °



1-Napht-SBFd_{C-C}: 3.679 Å between 1 Phenyl and 1 Cyclopentadienyl unitsH₁: 3.569 Åd₁: 0.89 Åθ₁: 14.05 °H₂: 2.962 Åd₂: 2.18 Åθ₂: 36.38 °

1-Phen-SBF

d_{C-C} : 3.625 Å between 2 Phenyl units

H_1 : 3.28 Å

d_1 : 1.54 Å

θ_1 : 25.23 °

H_2 : 3.428 Å

d_2 : 1.18 Å

θ_2 : 18.97 °

1-Phen-SBF

d_{C-C} : 3.779 Å between 2 Phenyl units

H_1 : 3.636 Å

d_1 : 1.03 Å

θ_1 : 15.81 °

H_2 : 3.368 Å

d_2 : 1.714 Å

θ_2 : 26.97 °

1-Phen-SBF

d_{C-C} : 3.610 Å between 1 Phenyl and 1 Cyclopentadienyl units

H_1 : 3.428 Å

d_1 : 1.13 Å

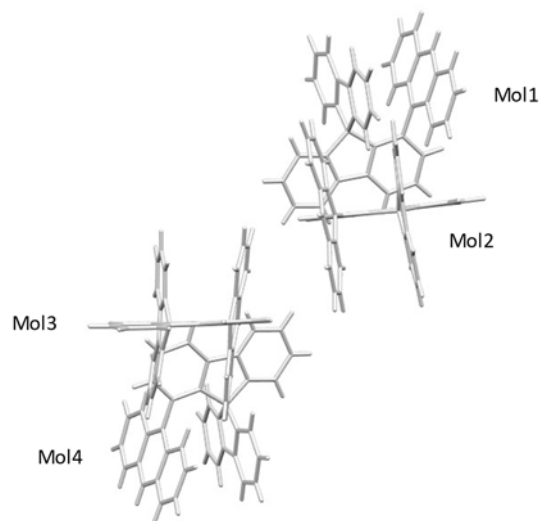
θ_1 : 18.27 °

H_2 : 3.138 Å

d_2 : 1.78 Å

θ_2 : 29.63 °

1-Anth-SBF



1-Anth-SBF (Mol1)

d_{C-C} : 3.766 Å between 2 Phenyl units

H_1 : 3.45 Å

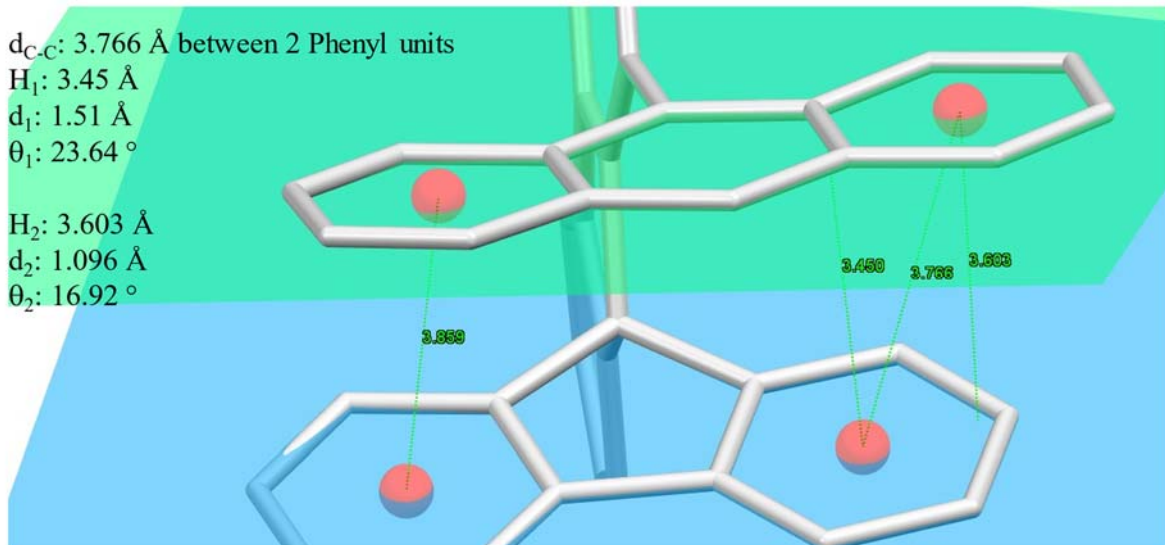
d_1 : 1.51 Å

θ_1 : 23.64 °

H_2 : 3.603 Å

d_2 : 1.096 Å

θ_2 : 16.92 °



1-Anth-SBF (Mol1)

d_{C-C} : 3.859 Å between 2 Phenyl units

H_1 : 3.787 Å

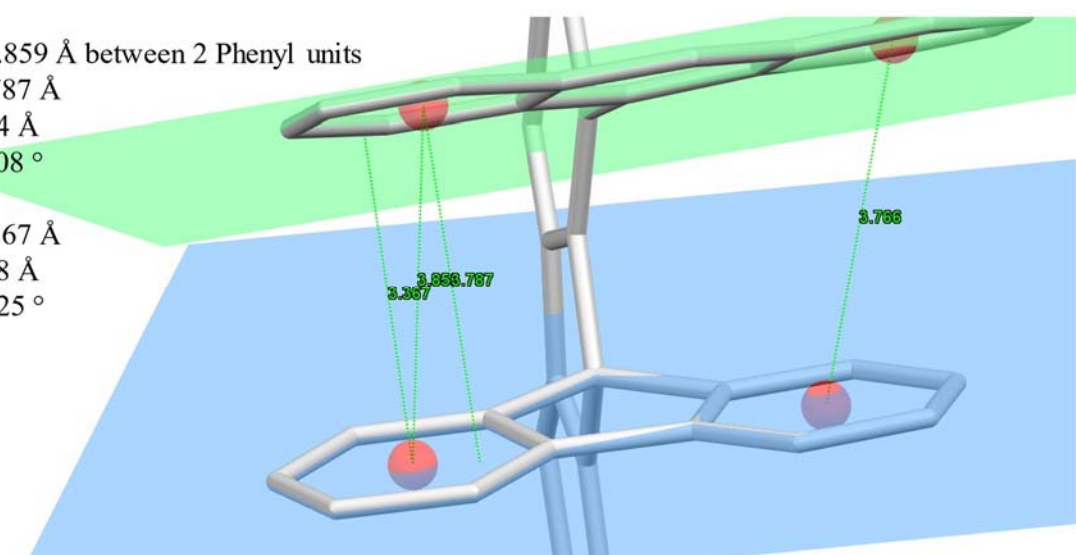
d_1 : 0.74 Å

θ_1 : 11.08 °

H_2 : 3.367 Å

d_2 : 1.88 Å

θ_2 : 29.25 °



1-Anth-SBF (Mol1)

d_{C-C} : 3.782 Å between 1 Phenyl and 1 Cyclopentadienyl units

H_1 : 3.647 Å

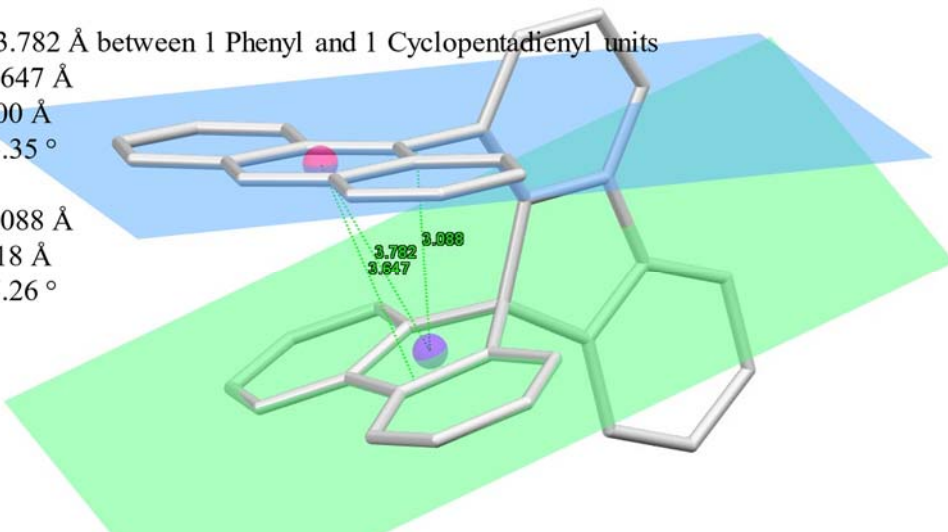
d_1 : 1.00 Å

θ_1 : 15.35 °

H_2 : 3.088 Å

d_2 : 2.18 Å

θ_2 : 35.26 °



1-Anth-SBF (Mol2)

d_{C-C} : 3.74 Å between 2 Phenyl units

H_1 : 3.359 Å

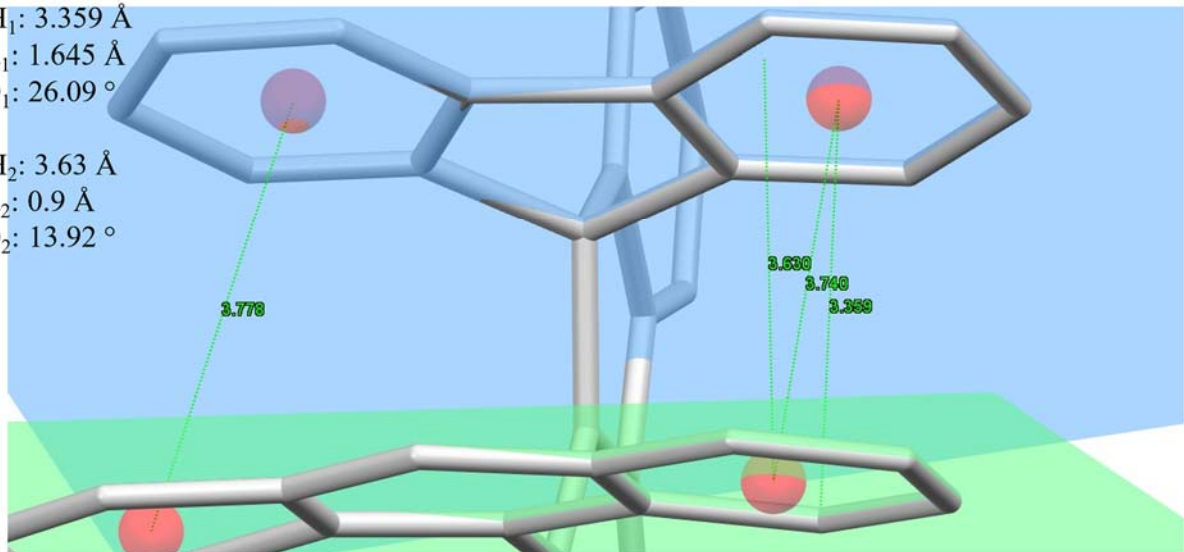
d_1 : 1.645 Å

θ_1 : 26.09 °

H_2 : 3.63 Å

d_2 : 0.9 Å

θ_2 : 13.92 °



1-Anth-SBF (Mol2)

d_{C-C} : 3.778 Å between 2 Phenyl units

H_1 : 3.689 Å

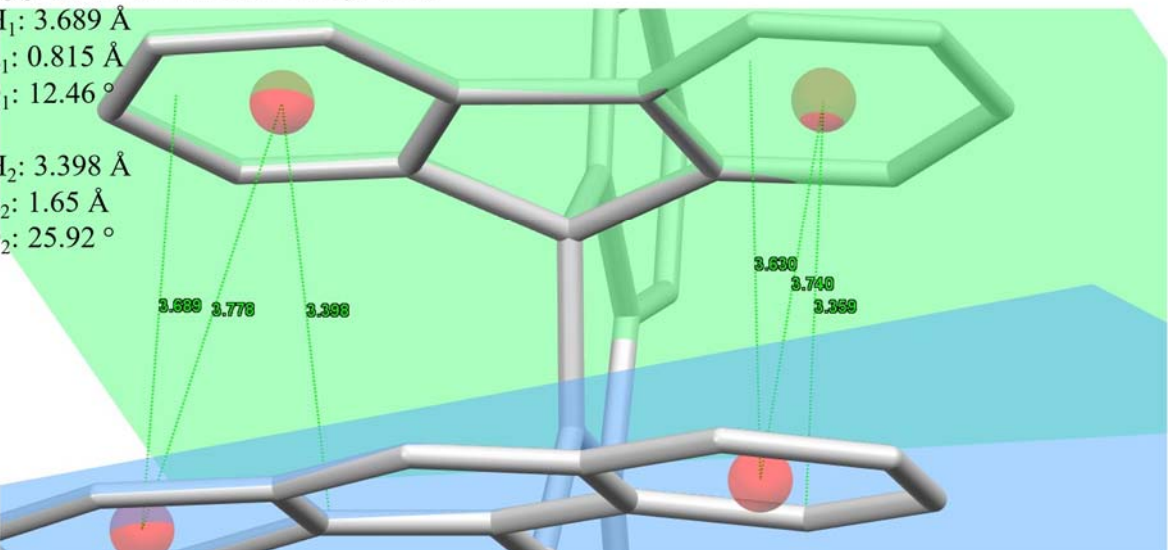
d_1 : 0.815 Å

θ_1 : 12.46 °

H_2 : 3.398 Å

d_2 : 1.65 Å

θ_2 : 25.92 °



1-Anth-SBF (Mol2)

d_{C-C} : 3.698 Å between 1 Phenyl and 1 Cyclopentadienyl units

H_1 : 3.512 Å

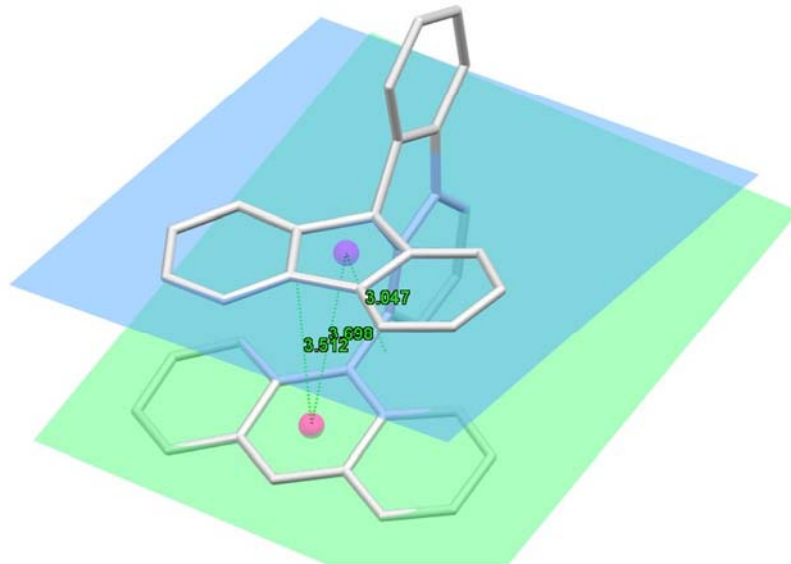
d_1 : 1.16 Å

θ_1 : 18.25 °

H_2 : 3.047 Å

d_2 : 2.09 Å

θ_2 : 34.5 °



1-Anth-SBF (Mol3)

d_{C-C} : 3.576 Å between 2 Phenyl units

H_1 : 3.497 Å

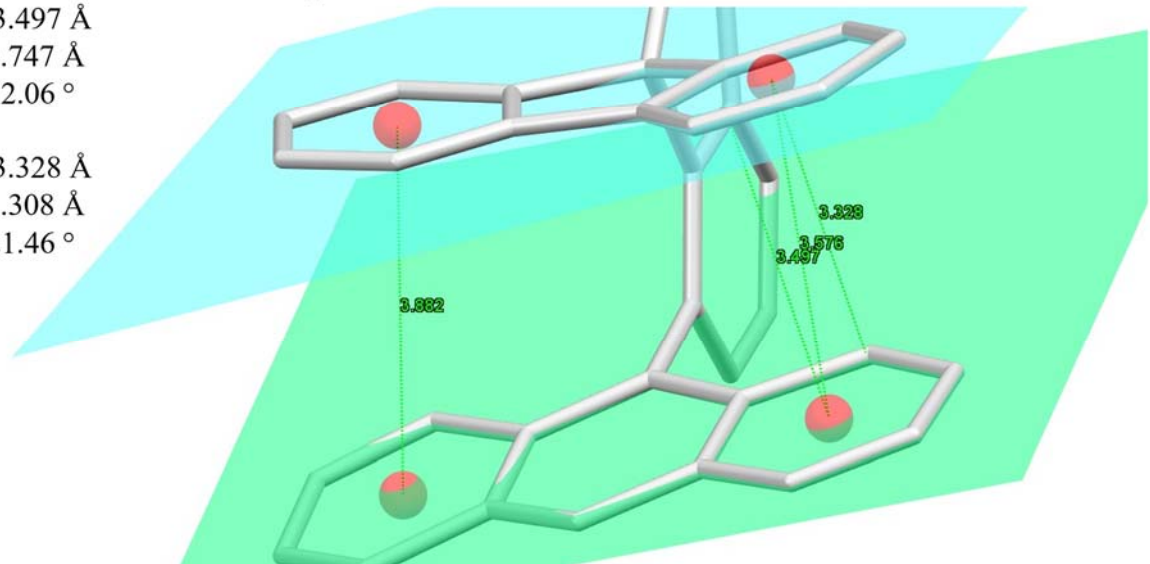
d_1 : 0.747 Å

θ_1 : 12.06 °

H_2 : 3.328 Å

d_2 : 1.308 Å

θ_2 : 21.46 °



1-Anth-SBF (Mol3)

d_{C-C} : 3.882 Å between 2 Phenyl units

H_1 : 3.84 Å

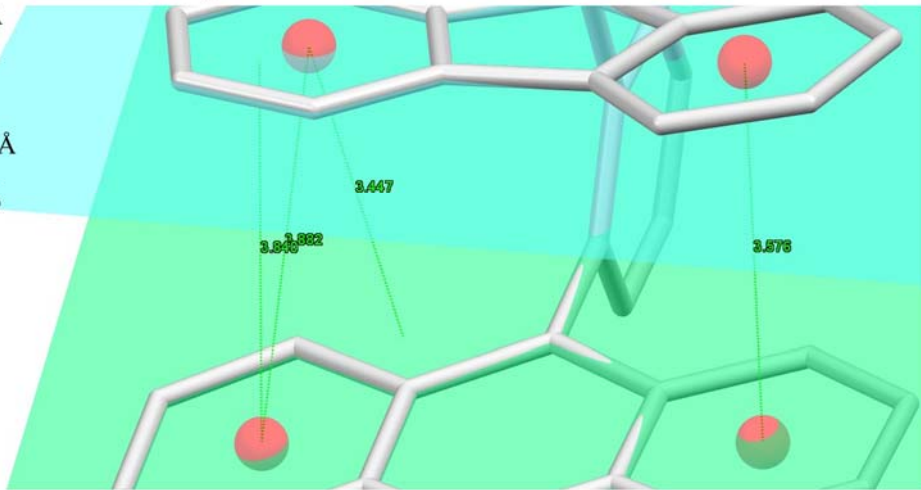
d_1 : 0.57 Å

θ_1 : 8.44 °

H_2 : 3.447 Å

d_2 : 1.79 Å

θ_2 : 27.38 °



1-Anth-SBF (Mol3)

d_{C-C} : 3.703 Å between 1 Phenyl and 1 Cyclopentadienyl units

H_1 : 3.045 Å

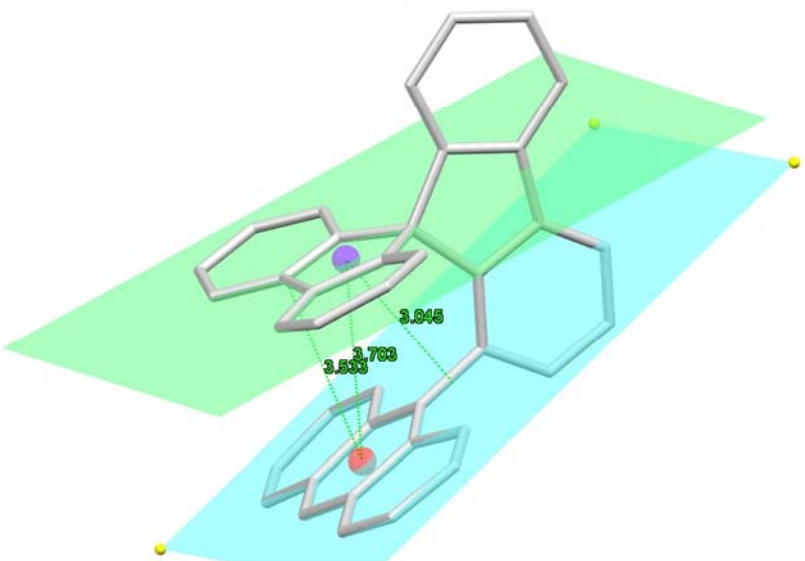
d_1 : 2.11 Å

θ_1 : 34.68 °

H_2 : 3.533 Å

d_2 : 1.11 Å

θ_2 : 17.43°



1-Anth-SBF (Mol4)

d_{C-C} : 3.759 Å between 2 Phenyl units

H_1 : 3.719 Å

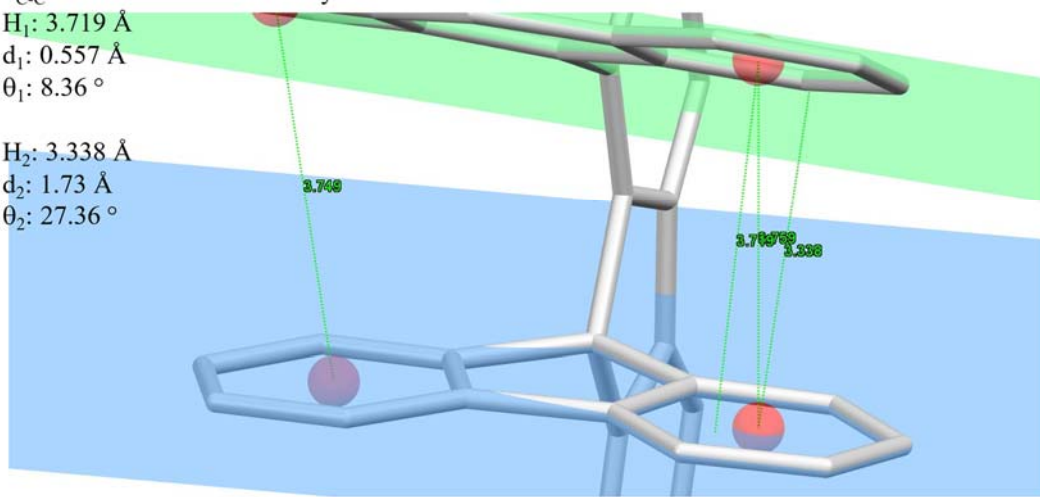
d_1 : 0.557 Å

θ_1 : 8.36 °

H_2 : 3.338 Å

d_2 : 1.73 Å

θ_2 : 27.36 °



1-Anth-SBF (Mol4)

d_{C-C} : 3.749 Å between 2 Phenyl units

H_1 : 3.697 Å

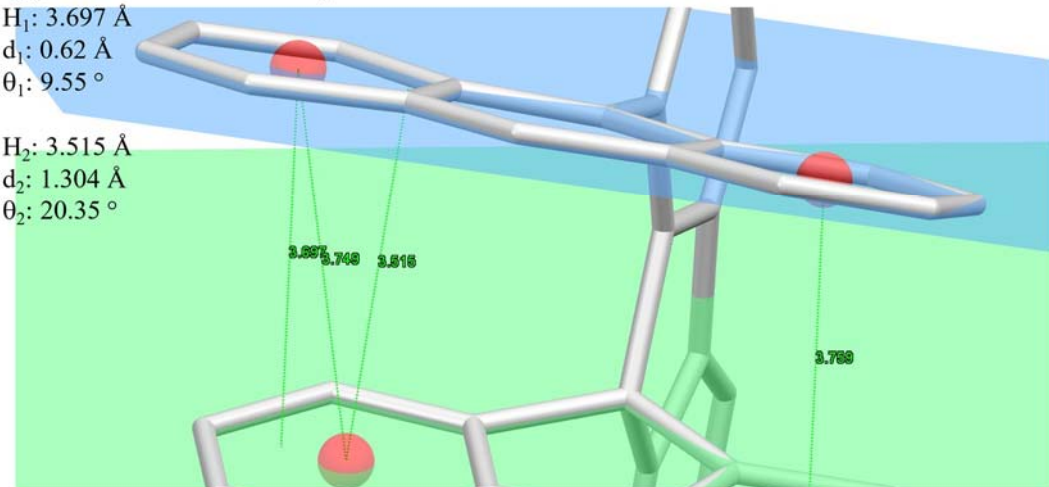
d_1 : 0.62 Å

θ_1 : 9.55 °

H_2 : 3.515 Å

d_2 : 1.304 Å

θ_2 : 20.35 °



1-Anth-SBF (Mol4)

d_{C-C} : 3.741 Å between 1 Phenyl and 1 Cyclopentadienyl units

H_1 : 3.098 Å

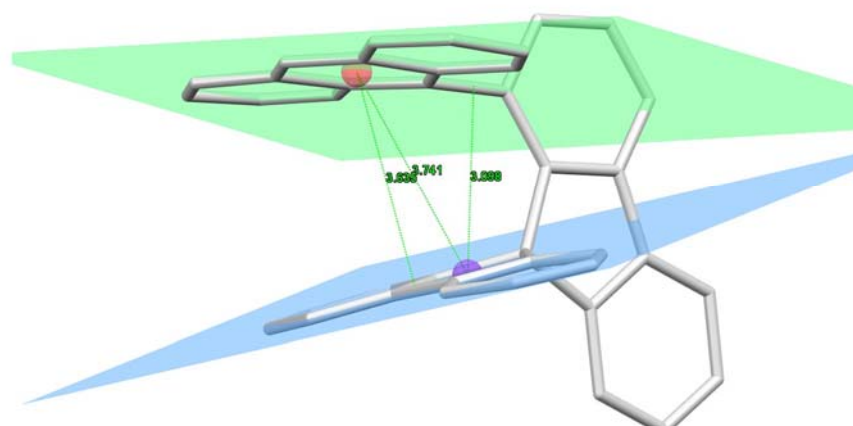
d_1 : 2.1 Å

θ_1 : 34.09 °

H_2 : 3.635 Å

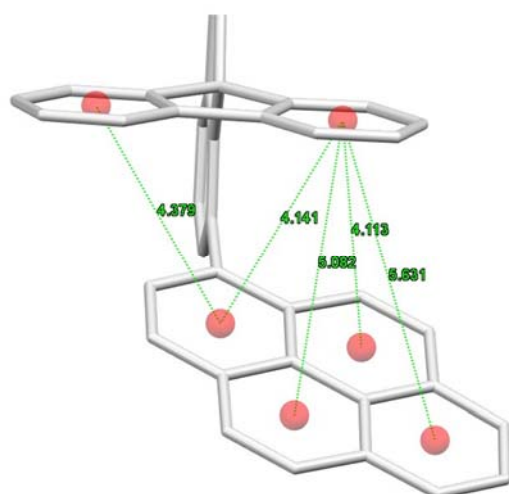
d_2 : 0.88 Å

θ_2 : 13.67 °



1-Pyr-SBF

No $d_{C-C} < 4 \text{ \AA}$



1-Pyr-SBF

d_{C-C} : 3.763 Å between 1 Phenyl and 1 Cyclopentadienyl units

H_1 : 3.065 Å

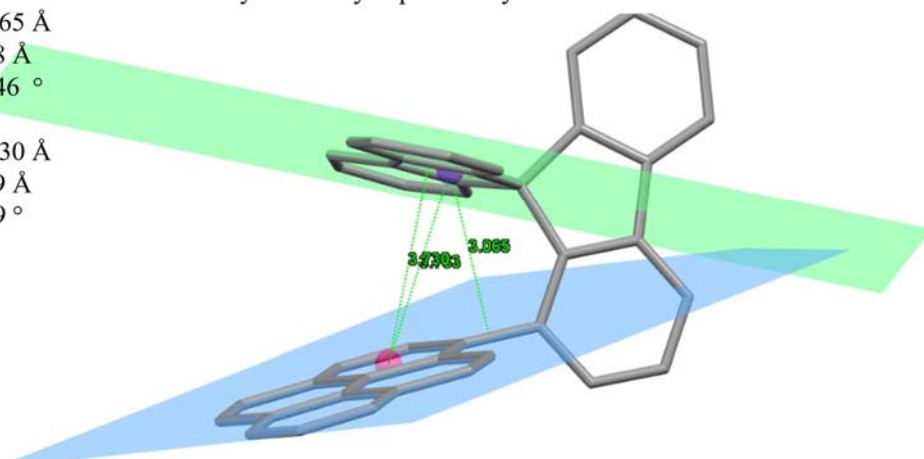
d_1 : 2.18 Å

θ_1 : 35.46 °

H_2 : 3.730 Å

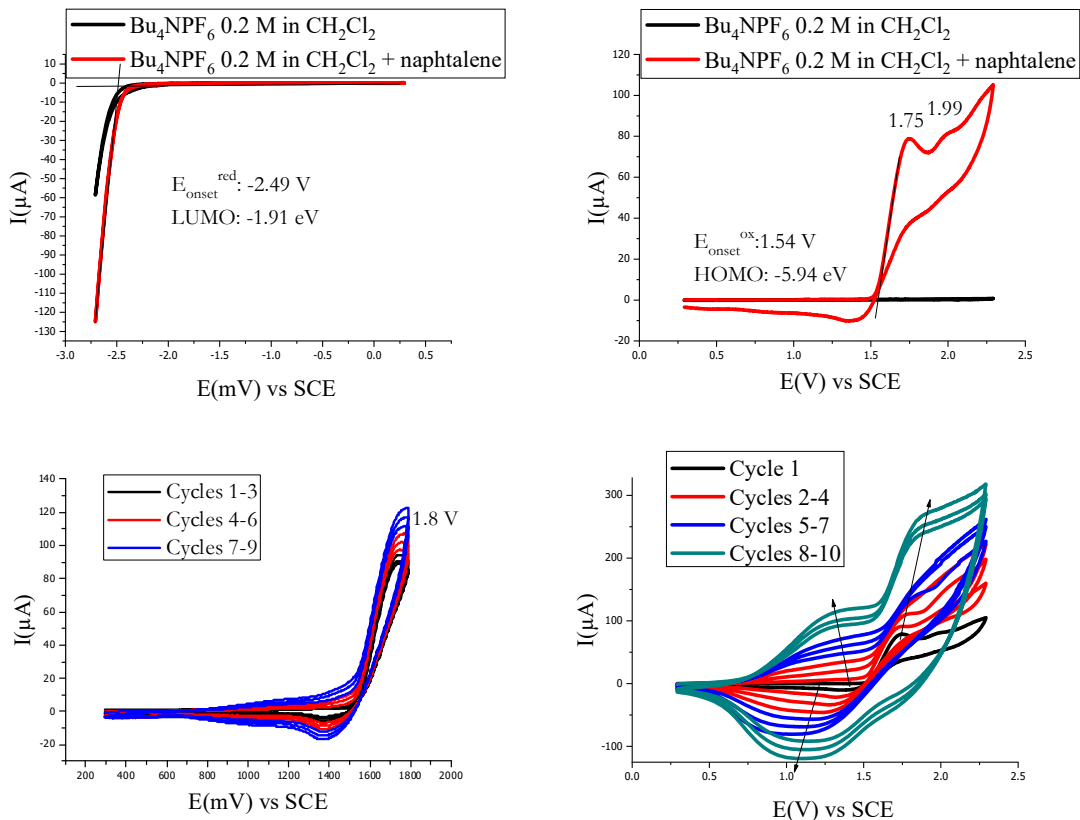
d_2 : 0.49 Å

θ_2 : 7.59 °



4 Electrochemistry

Naphthalene

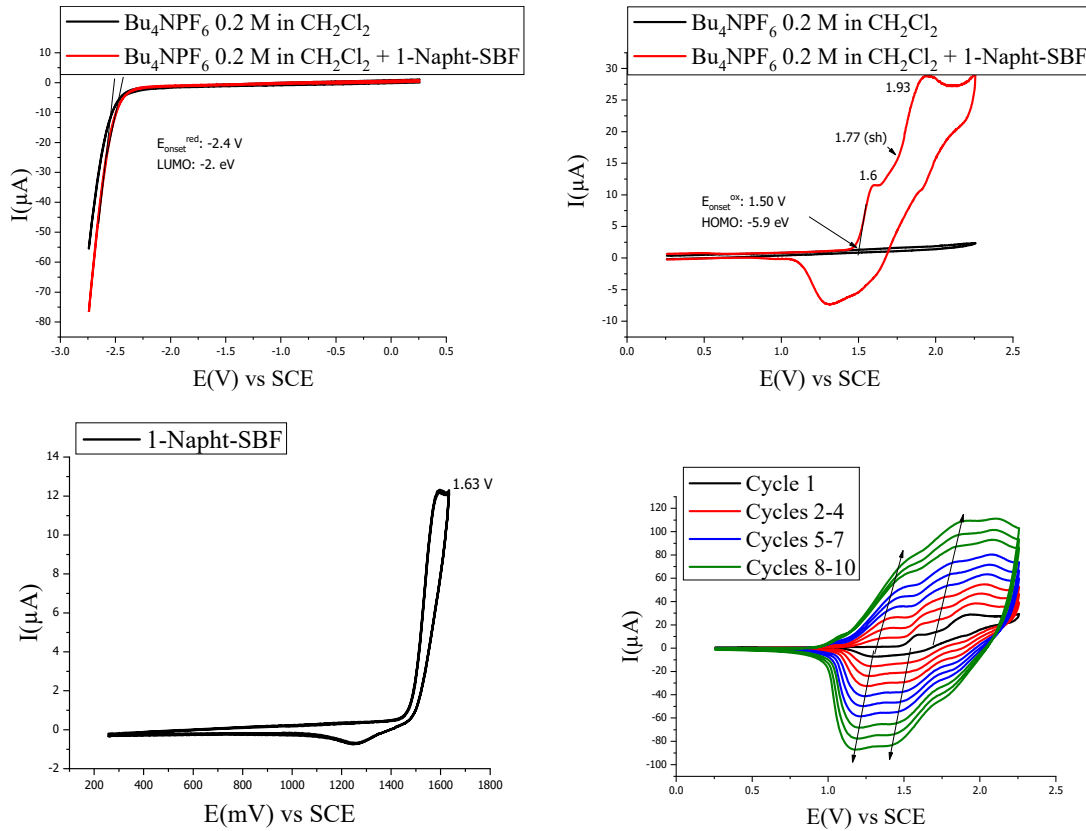


Cyclic voltammetries (Bu_4NPF_6 0.2 M / CH_2Cl_2 , sweep-rate 100 mV s⁻¹, platinum disk working electrode diameter 1mm) in presence of **Naphthalene** in concentration $1.25 \times 10^{-2} \text{ M}$.

Top Left in reduction up to -2.71 V and **Top Right** in oxidation up to 2.30 V.

Bottom Left in oxidation: nine cycles up to 1.8 V and **Bottom Right** ten cycles in oxidation up to 2.3 V showing a weak (**left**) or an intense (**right**) electrodeposition process.

1-Napht-SBF

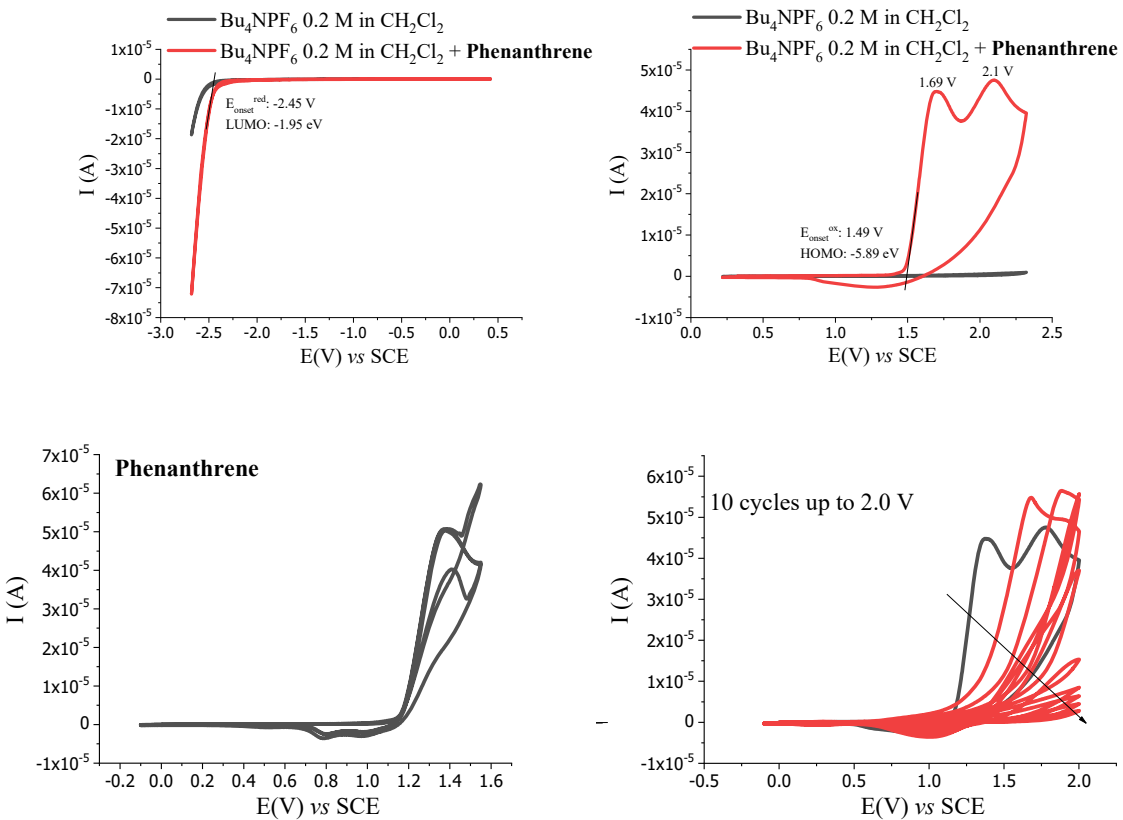


Cyclic voltammetries (Bu_4NPF_6 0.2 M / CH_2Cl_2 , sweep-rate 100 mV s⁻¹, platinum disk working electrode diameter 1mm) in presence of **1-Napht-SBF** in concentration 3.04×10^{-3} M.

Top Left in reduction up to -2.75 V and **Top Right** in oxidation up to 2.27 V.

Bottom Left in oxidation: three cycles up to 1.63 V and **Bottom Right** ten cycles in oxidation up to 2.26 V showing an intense electrodeposition process.

Phenanthrene

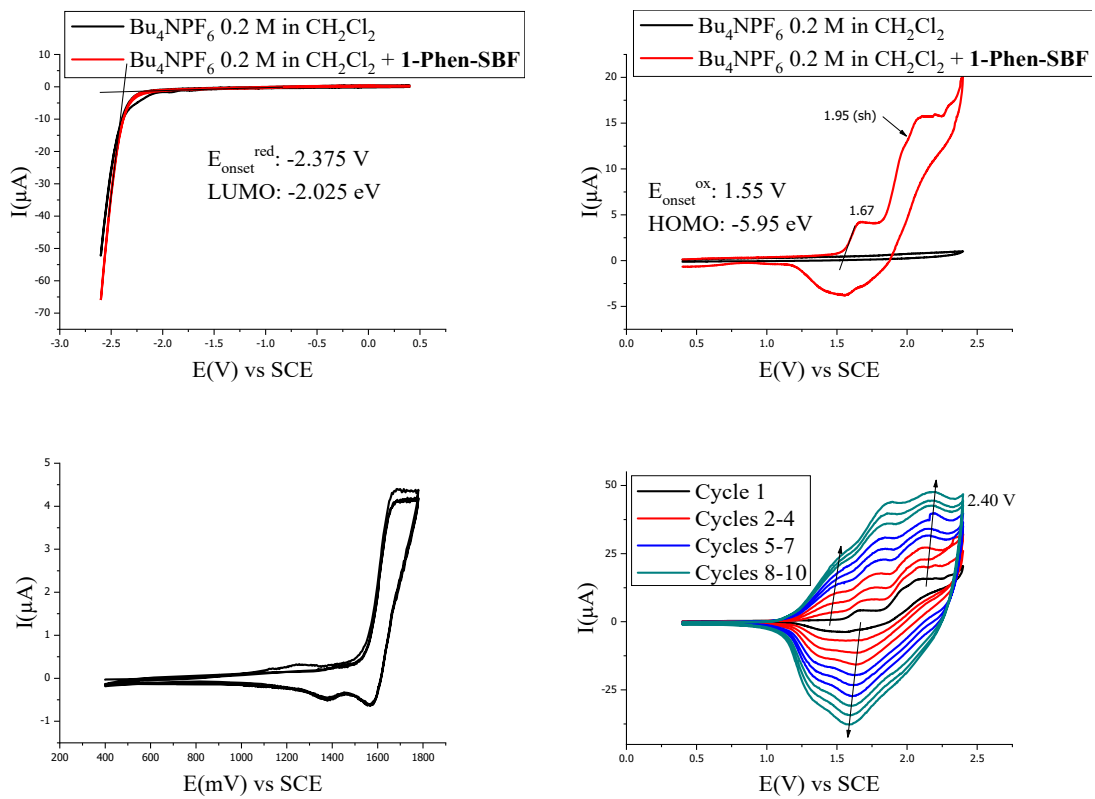


Cyclic voltammetries (Bu_4NPF_6 0.2 M / CH_2Cl_2 , sweep-rate 100 mV s⁻¹, platinum disk working electrode diameter 1mm) in presence of **Phenanthrene** in concentration $6.9 \cdot 10^{-3}$ M.

Top Left in reduction up to -2.7 V and **Top Right** in oxidation up to 2.3 V.

Bottom Left in oxidation: three cycles up to 1.55 V and **Bottom Right** ten cycles in oxidation up to 2.0 V showing an overoxidation process.

1-Phen-SBF

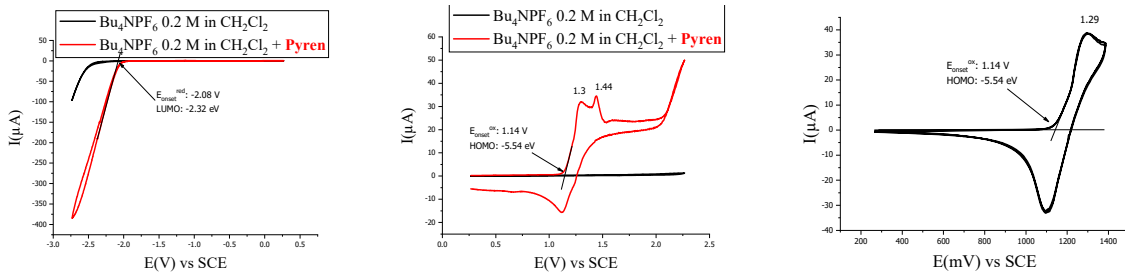


Cyclic voltammetries (Bu_4NPF_6 0.2 M / CH_2Cl_2 , sweep-rate 100 mV s^{-1} , platinum disk working electrode diameter 1mm) in presence of **1-Phen-SBF** in concentration 2×10^{-3} M.

Top Left in reduction up to -2.6 V and **Top Right** in oxidation up to 2.4 V.

Bottom Left in oxidation: three cycles up to 1.77 V and **Bottom Right** ten cycles in oxidation up to 2.40 V showing an intense electrodeposition process.

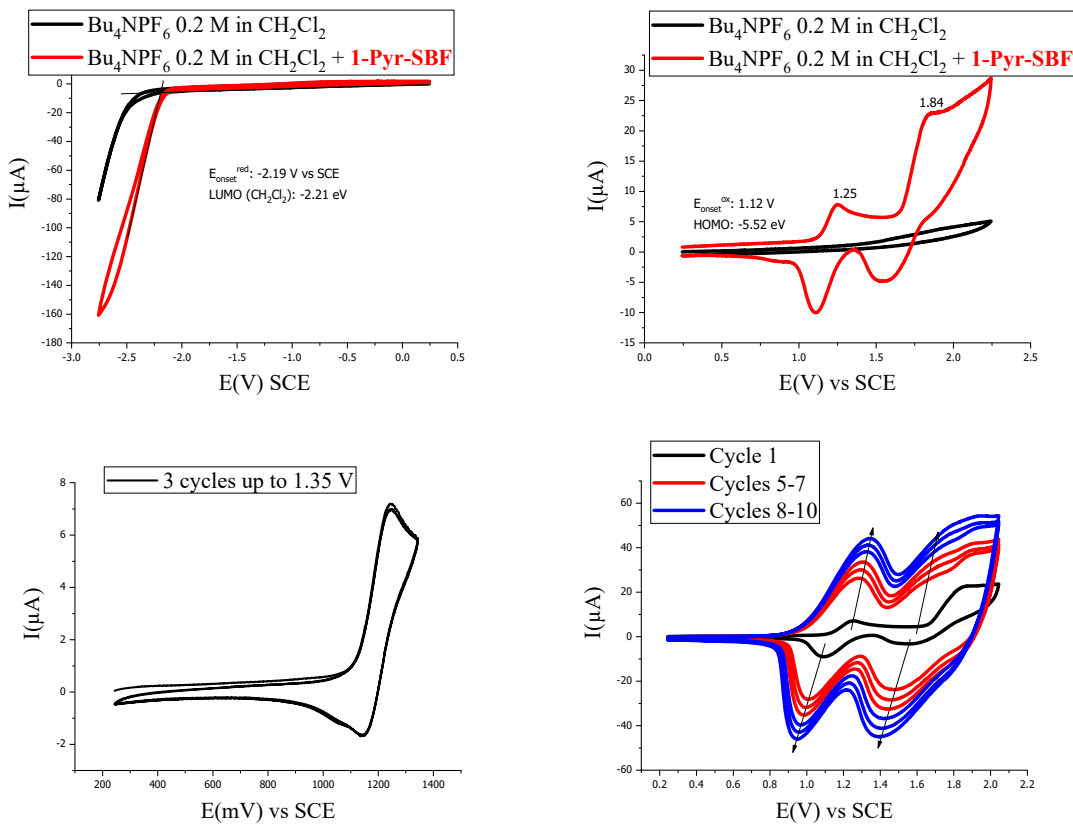
Pyrene



Cyclic voltammetries (Bu_4NPF_6 0.2 M / CH_2Cl_2 , sweep-rate 100 mV s⁻¹, platinum disk working electrode diameter 1mm) in presence of **Pyrene** in concentration 1.25×10^{-2} M.

Left in reduction up to -2.73 V, **Middle** in oxidation up to 2.27 V and **Right** in oxidation up to 1.39 V.

1-Pyr-SBF

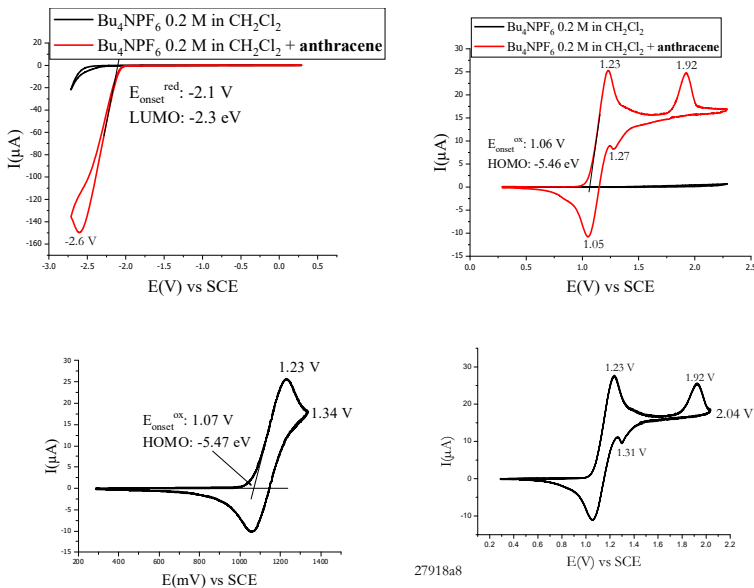


Cyclic voltammetries (Bu_4NPF_6 0.2 M / CH_2Cl_2 , sweep-rate 100 mV s⁻¹, platinum disk working electrode diameter 1mm) in presence of **1-Pyr-SBF** in concentration 2.47×10^{-3} M.

Top Left in reduction up to -2.76 V and **Top Right** in oxidation up to 2.26 V.

Bottom Left in oxidation: three cycles up to 1.34 V and **Bottom Right** ten cycles in oxidation up to 2.05 V showing an electrodeposition process.

Anthracene

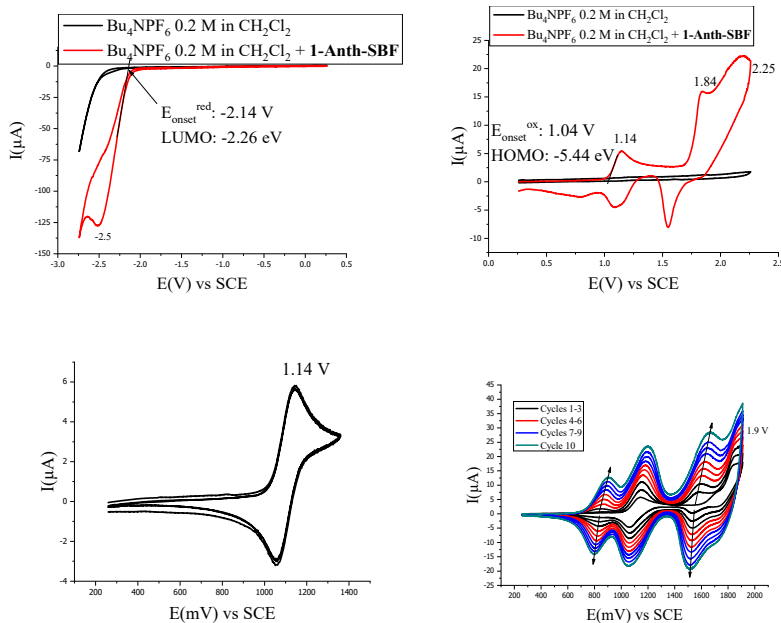


Cyclic voltammetries (Bu_4NPF_6 0.2 M / CH_2Cl_2 , sweep-rate 100 mV s⁻¹, platinum disk working electrode diameter 1mm) in presence of **Anthracene** in concentration 4.43×10^{-3} M.

Top Left in reduction up to -2.72 V and **Top Right** in oxidation up to 2.30 V.

Bottom Left in oxidation: three cycles up to 1.34 V and **Bottom Right** three cycles in oxidation up to 2.04 V (no electrodeposition process).

1-Anth-SBF

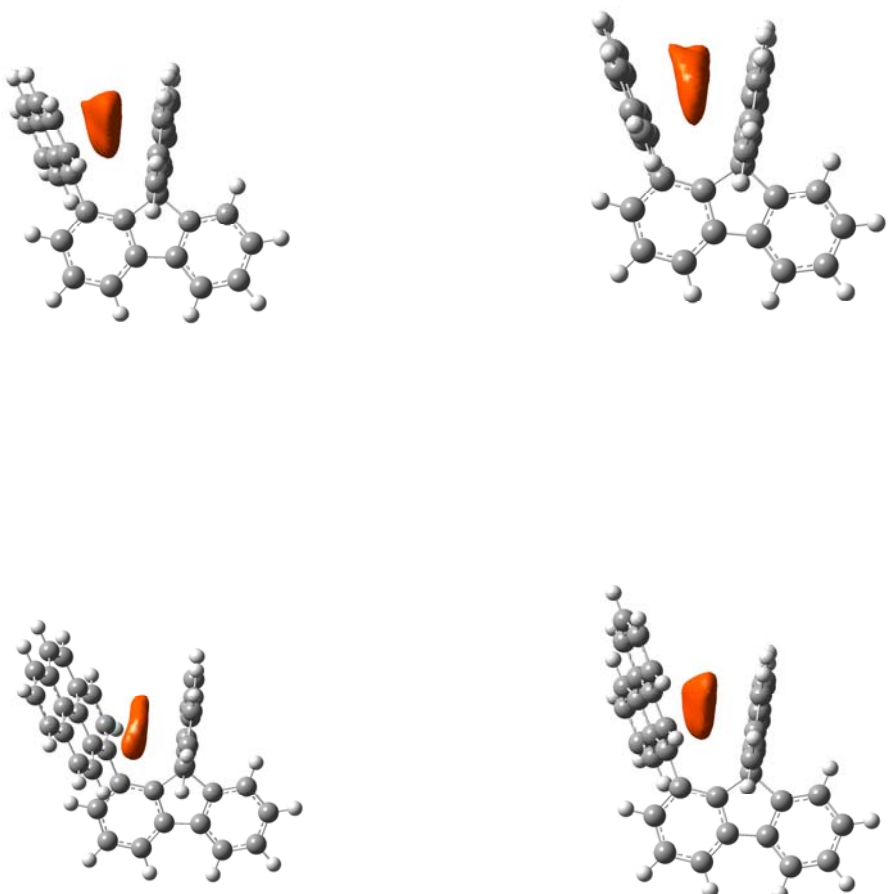


Cyclic voltammetries (Bu_4NPF_6 0.2 M / CH_2Cl_2 , sweep-rate 100 mV s⁻¹, platinum disk working electrode diameter 1mm) in presence of **1-Anth-SBF** in concentration 2.16×10^{-3} M.

Top Left in reduction up to -2.74 V and **Top Right** in oxidation up to 2.25 V.

Bottom Left in oxidation: three cycles up to 1.36 V and **Bottom Right** ten cycles in oxidation up to 1.9 V showing an intense electrodeposition process.

5 Molecular modelling



Electrostatic potential surfaces of **1-Naph-SBF**, **1-Anth-SBF**, **1-Phen-SBF**, **1-Pyr-SBF**
(orange=negative regions, positive regions have been omitted for clarity, density: 0.03)

Table S 1. TD-DFT results on **1-Naph-SBF** (*b3lyp*, *6-311+g(d,p)*)

Wavelength (nm)	Oscillator Strength	Major contribs
308	0.0016	H-1→LUMO (61%), HOMO→LUMO (35%)
304	0.041	H-1→L+1 (83%)
304	0.061	HOMO→L+1 (87%)
301	0.0364	H-1→LUMO (23%), HOMO→LUMO (41%), HOMO→L+2 (14%)
299	0.0478	HOMO→L+2 (79%)
296	0.0475	H-1→L+2 (84%)
287	0.0261	H-2→LUMO (64%)

282	0.0034	H-4→LUMO (12%), H-3→LUMO (16%), H-2→LUMO (12%), H-1→L+3 (12%), HOMO→L+4 (18%), HOMO→L+5 (12%)
282	0.0003	H-2→LUMO (13%), H-1→L+3 (16%), HOMO→L+3 (56%)
278	0.0364	H-2→L+1 (12%), H-1→L+4 (45%), HOMO→L+4 (14%)
277	0.0929	H-2→L+1 (64%), H-1→L+3 (12%), H-1→L+4 (12%)
274	0.0387	H-1→L+3 (44%), HOMO→L+3 (20%), HOMO→L+4 (14%)
272	0.0922	H-2→L+2 (83%)
269	0.0375	H-1→L+4 (17%), HOMO→L+4 (41%)
264	0.0644	H-2→L+3 (56%)
263	0.0043	H-5→L+2 (12%), H-2→L+3 (18%), H-1→L+5 (23%), HOMO→L+5 (14%)
259	0.005	H-6→L+1 (23%), H-5→L+2 (15%), H-2→L+4 (20%)
259	0.0345	H-2→L+4 (54%)
256	0.0106	H-6→LUMO (10%), H-4→LUMO (39%), H-3→LUMO (37%)
252	0.0208	H-5→L+2 (10%), H-1→L+5 (34%), H-1→L+6 (14%)

Table S 2. TD-DFT results on **1-Anth-SBF** (*b3lyp*, 6-311+g(*d,p*))

Wavelength (nm)	Oscillator Strength	Major contribs
403	0.0819	HOMO→LUMO (98%)
365	0.0007	H-1→LUMO (97%)
349	0.0012	HOMO→L+1 (93%)
336	0.0013	H-2→LUMO (77%)
335	0.0038	HOMO→L+2 (92%)
324	0.0001	H-4→LUMO (25%), H-3→LUMO (14%), H-2→LUMO (13%), HOMO→L+3 (16%), HOMO→L+5 (28%)
313	0.0016	HOMO→L+3 (78%), HOMO→L+5 (10%)
308	0.0323	H-1→L+1 (95%)
302	0.0079	HOMO→L+4 (95%)
299	0.0006	H-4→LUMO (24%), H-3→LUMO (63%)
294	0.0343	H-1→L+2 (81%)
289	0.0011	H-5→LUMO (97%)
285	0.0002	H-1→L+3 (84%)
282	0.0002	H-7→LUMO (20%), H-6→LUMO (70%)
280	0.1754	H-2→L+1 (82%)
279	0.0024	H-1→L+4 (67%)
277	0.0176	H-7→LUMO (14%), HOMO→L+5 (10%), HOMO→L+6 (23%), HOMO→L+7 (21%)
274	0.0066	H-7→LUMO (22%), H-6→LUMO (11%), HOMO→L+6 (30%), HOMO→L+7 (12%)
272	0.0259	H-2→L+2 (70%), HOMO→L+6 (18%)
269	0.0876	H-2→L+3 (68%), H-1→L+3 (11%)

Table S 3. TD-DFT results on **1-Phen-SBF** (b3lyp, 6-311+g(d,p))

Wavelength (nm)	Oscillator Strength	Major contribs
323	0.0078	H-2→LUMO (10%), HOMO→LUMO (15%), HOMO→L+1 (35%), HOMO→L+3 (11%)
313	0.0386	H-1→LUMO (61%), HOMO→LUMO (28%)
310	0.0265	H-1→LUMO (31%), HOMO→LUMO (41%), HOMO→L+1 (13%)
304	0.0102	HOMO→L+2 (82%)
302	0.0489	H-1→L+1 (75%)
299	0.0161	H-1→L+1 (12%), HOMO→L+1 (19%), HOMO→L+3 (46%)
298	0.0462	H-1→L+2 (80%)
289	0.0435	H-3→LUMO (17%), H-2→LUMO (23%), H-1→L+3 (30%)
286	0.0195	H-3→LUMO (14%), H-2→LUMO (20%), H-1→L+3 (53%)
283	0.0917	H-2→LUMO (22%), H-1→L+4 (25%), HOMO→L+4 (31%)
281	0.085	H-3→LUMO (19%), H-2→LUMO (15%), H-2→L+1 (20%), H-1→L+4 (18%)
279	0.0094	H-2→L+1 (14%), H-1→L+4 (18%), H-1→L+5 (13%), HOMO→L+4 (34%)
278	0.0086	H-1→L+5 (54%)
276	0.0113	H-3→L+1 (13%), H-2→L+1 (11%), H-1→L+4 (15%), HOMO→L+4 (13%), HOMO→L+5 (28%)
275	0.0071	H-3→L+2 (11%), H-2→L+2 (70%)
275	0.0191	H-3→LUMO (11%), H-2→L+3 (10%), HOMO→L+5 (62%)
272	0.0747	H-3→L+2 (74%)
271	0.0202	H-3→L+1 (21%), H-2→L+1 (18%), H-2→L+3 (24%), HOMO→L+3 (15%)
265	0.0719	H-3→L+3 (37%), H-2→L+3 (10%), H-2→L+4 (13%)
263	0.1138	H-3→L+3 (21%), H-3→L+4 (11%), H-2→L+4 (26%)

Table S 4. TD-DFT results on **1-Pyre-SBF** (b3lyp, 6-311+g(d,p))

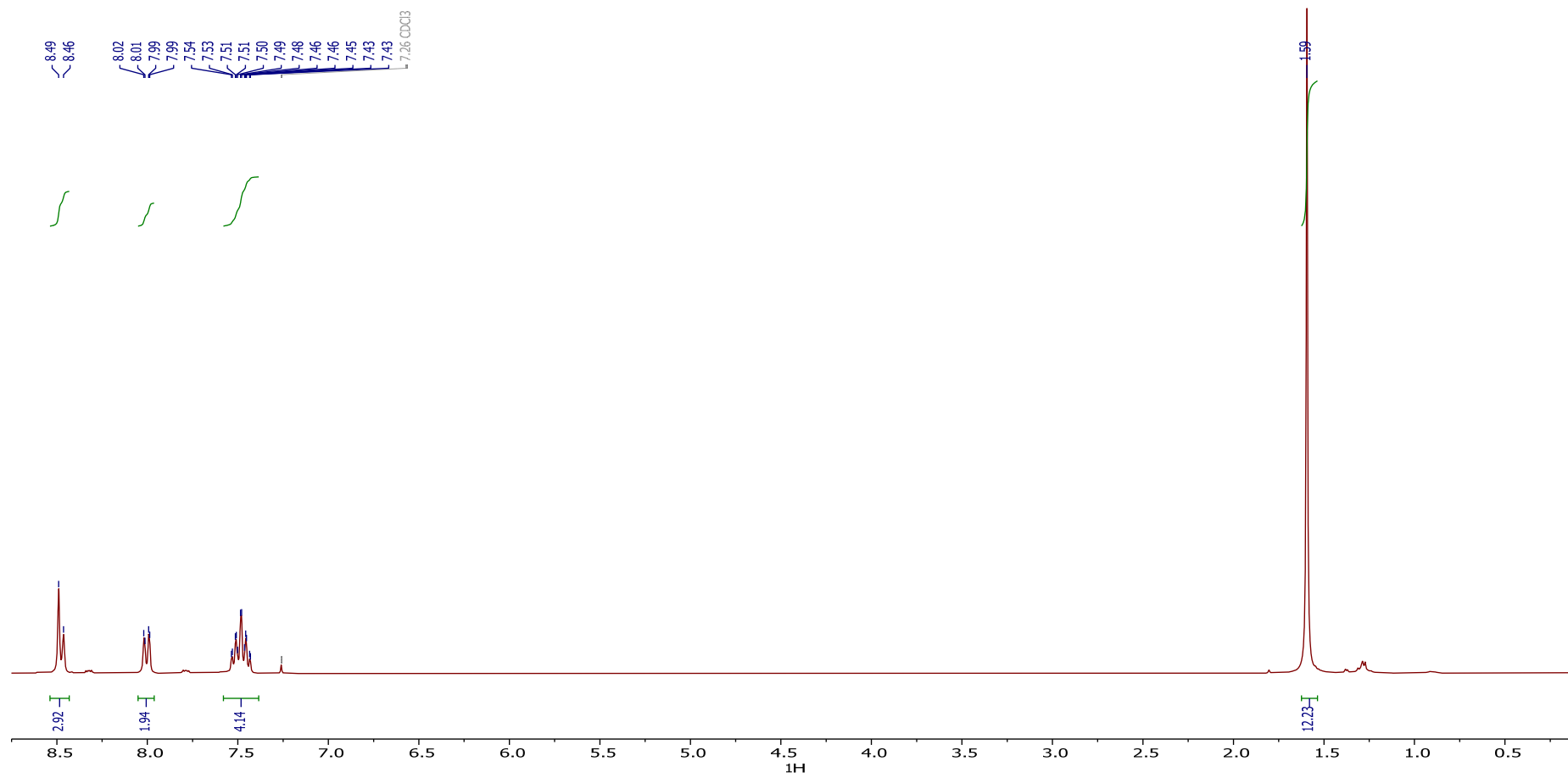
Wavelength (nm)	Oscillator Strength	Major contribs
355	0.3354	HOMO→LUMO (89%)
343	0.0024	H-3→LUMO (14%), H-2→LUMO (14%), H-1→LUMO (22%), HOMO→L+1 (25%), HOMO→L+3 (22%)
337	0.0279	H-1→LUMO (69%), HOMO→L+1 (21%)
329	0.0027	HOMO→L+1 (46%), HOMO→L+3 (25%)
327	0.0071	HOMO→L+2 (93%)
314	0.0112	H-3→LUMO (19%), H-2→LUMO (72%)
305	0.0460	H-1→L+1 (91%)
299	0.0009	HOMO→L+4 (92%)
297	0.0621	H-1→L+2 (77%)
294	0.0024	HOMO→L+5 (75%), HOMO→L+6 (12%)
290	0.0055	HOMO→L+5 (11%), HOMO→L+6 (69%)
283	0.1492	H-4→LUMO (30%), H-3→LUMO (27%), HOMO→L+3 (18%)

281	0.0092	H-2→L+1 (10%), H-1→L+4 (68%)
280	0.1703	H-4→LUMO (19%), H-2→L+1 (45%)
278	0.0375	H-7→LUMO (11%), H-5→LUMO (20%), H-4→LUMO (12%), H-2→L+1 (25%)
278	0.0030	H-1→L+3 (21%), H-1→L+5 (59%)
276	0.0827	H-2→L+2 (73%)
274	0.0081	H-7→LUMO (12%), H-6→LUMO (11%), H-5→LUMO (10%), H-1→L+3 (30%)
273	0.0625	H-7→LUMO (11%), H-4→LUMO (11%), H-1→L+3 (32%), H-1→L+5 (10%)
269	0.0191	H-7→LUMO (33%), H-5→LUMO (40%)

6 Copy of NMR spectra

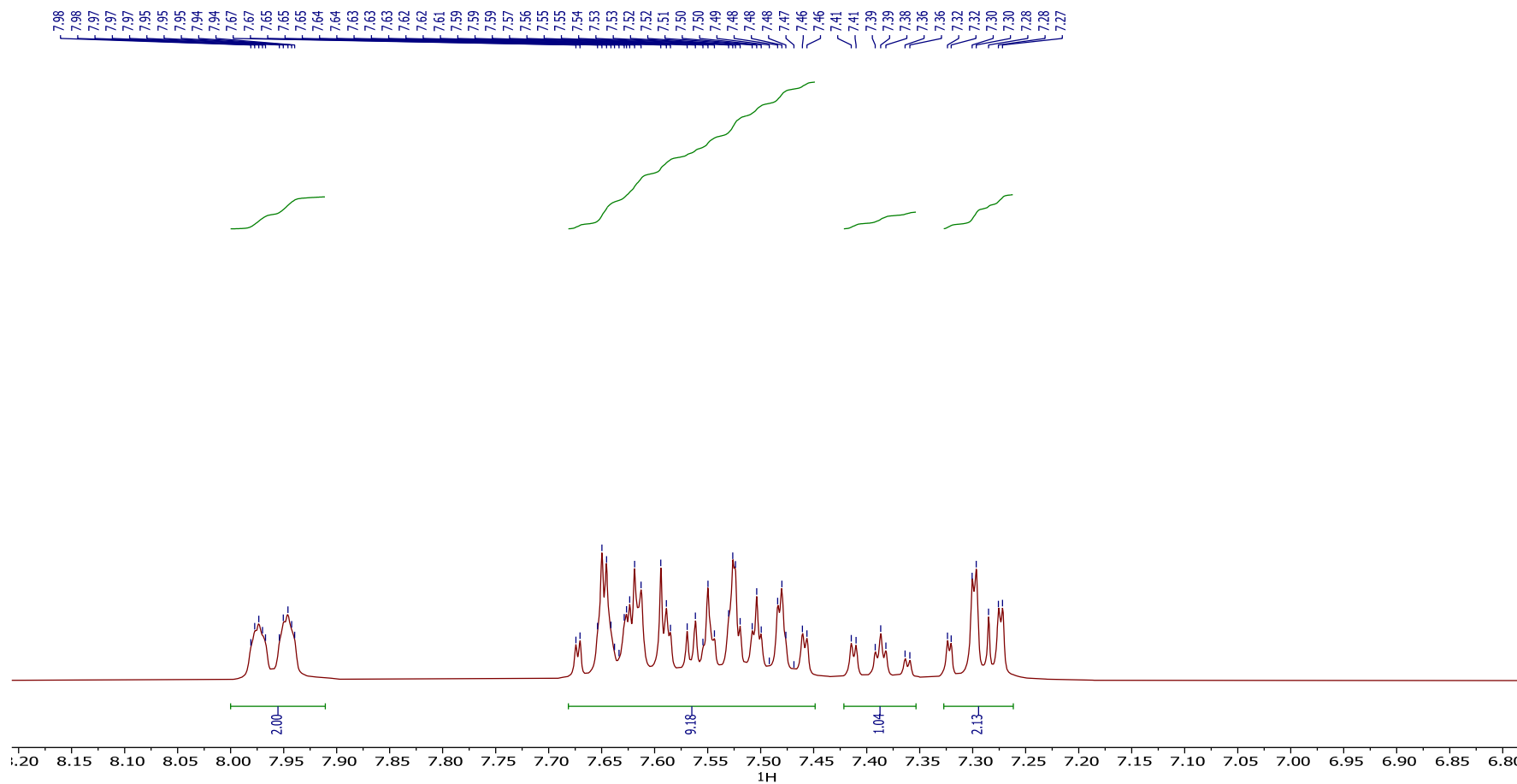
2-Bpin-Anth

^1H (CDCl_3)

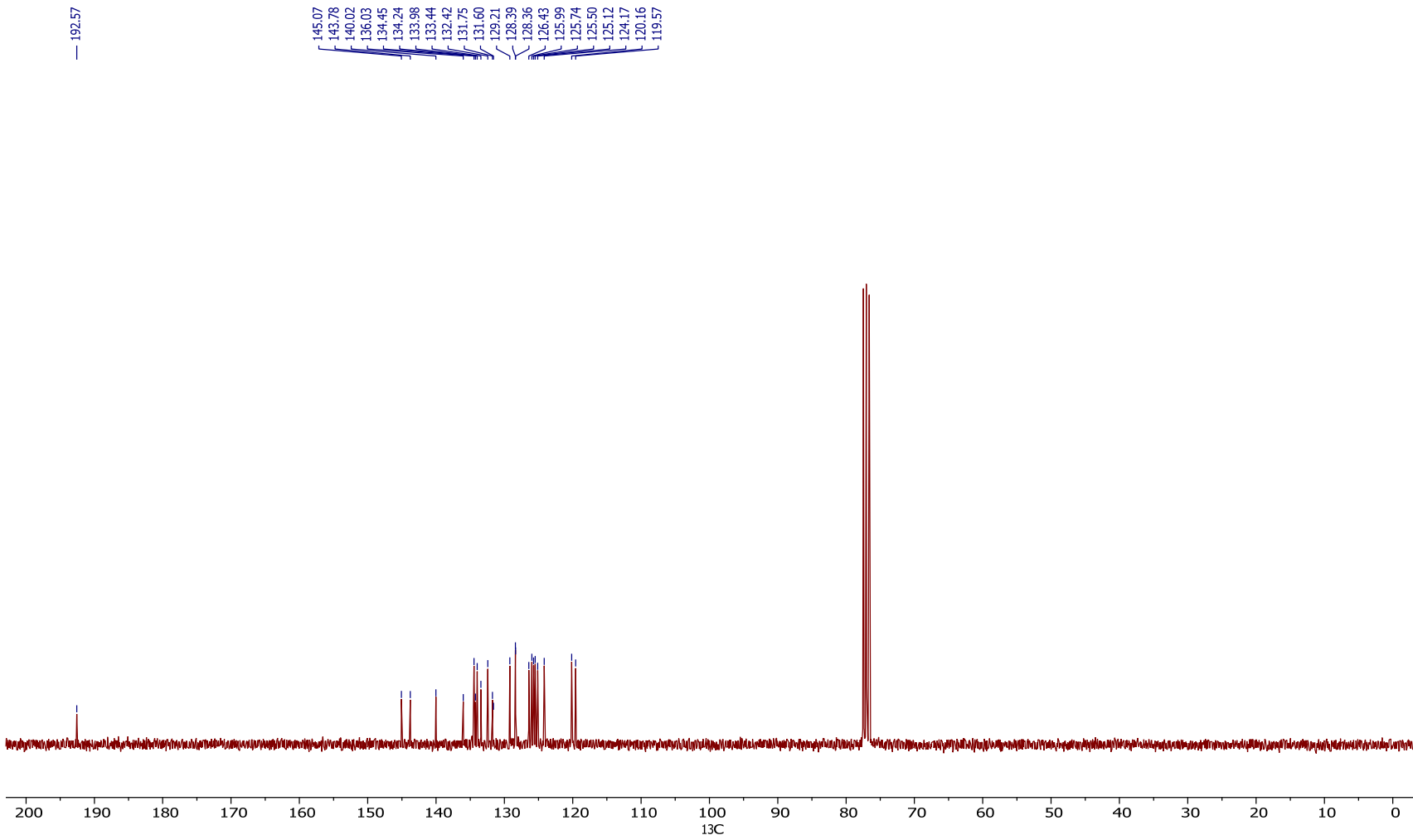


1-Napht-FO

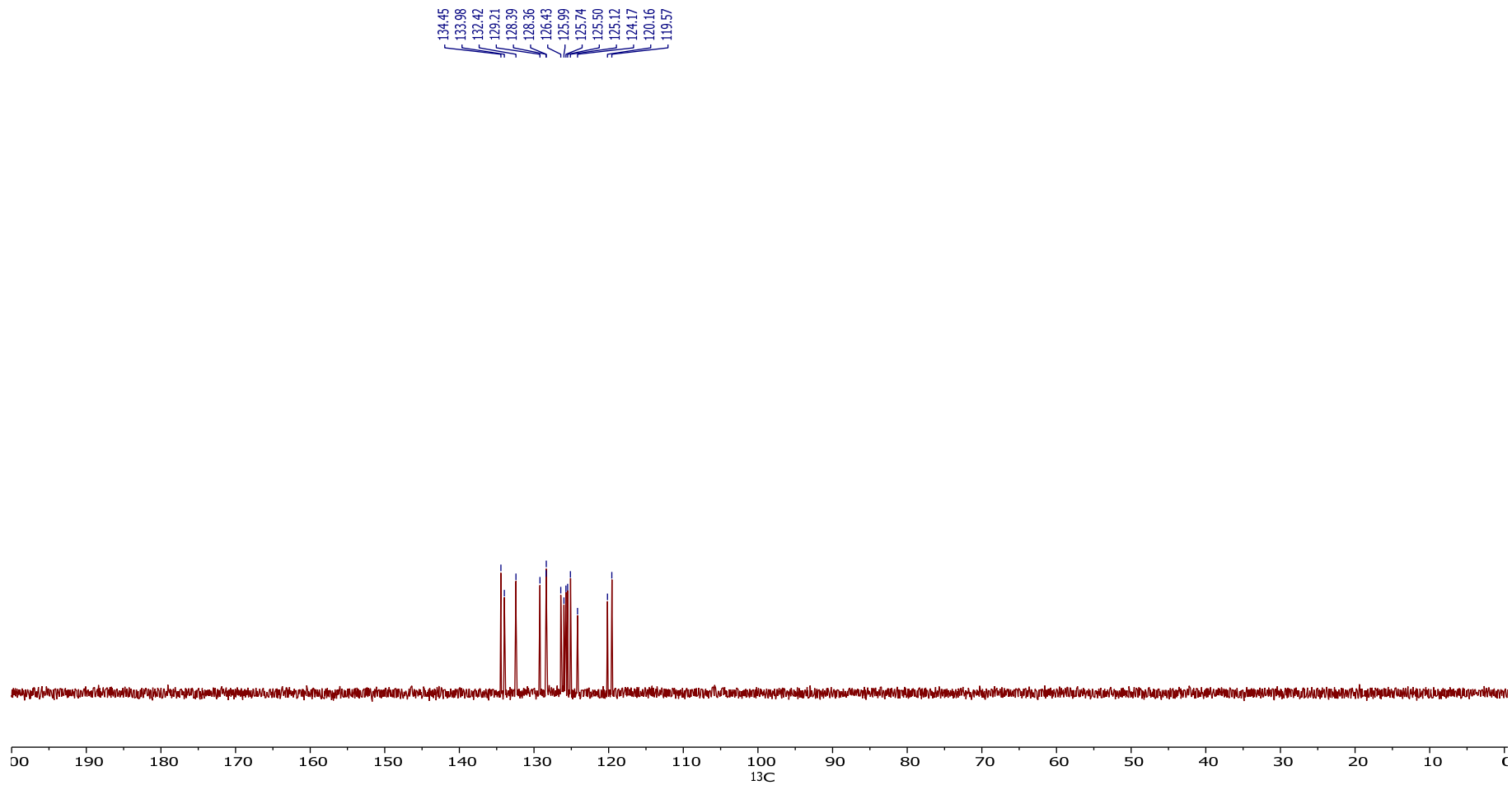
^1H (CD_2Cl_2)



¹³C (CDCl₃)

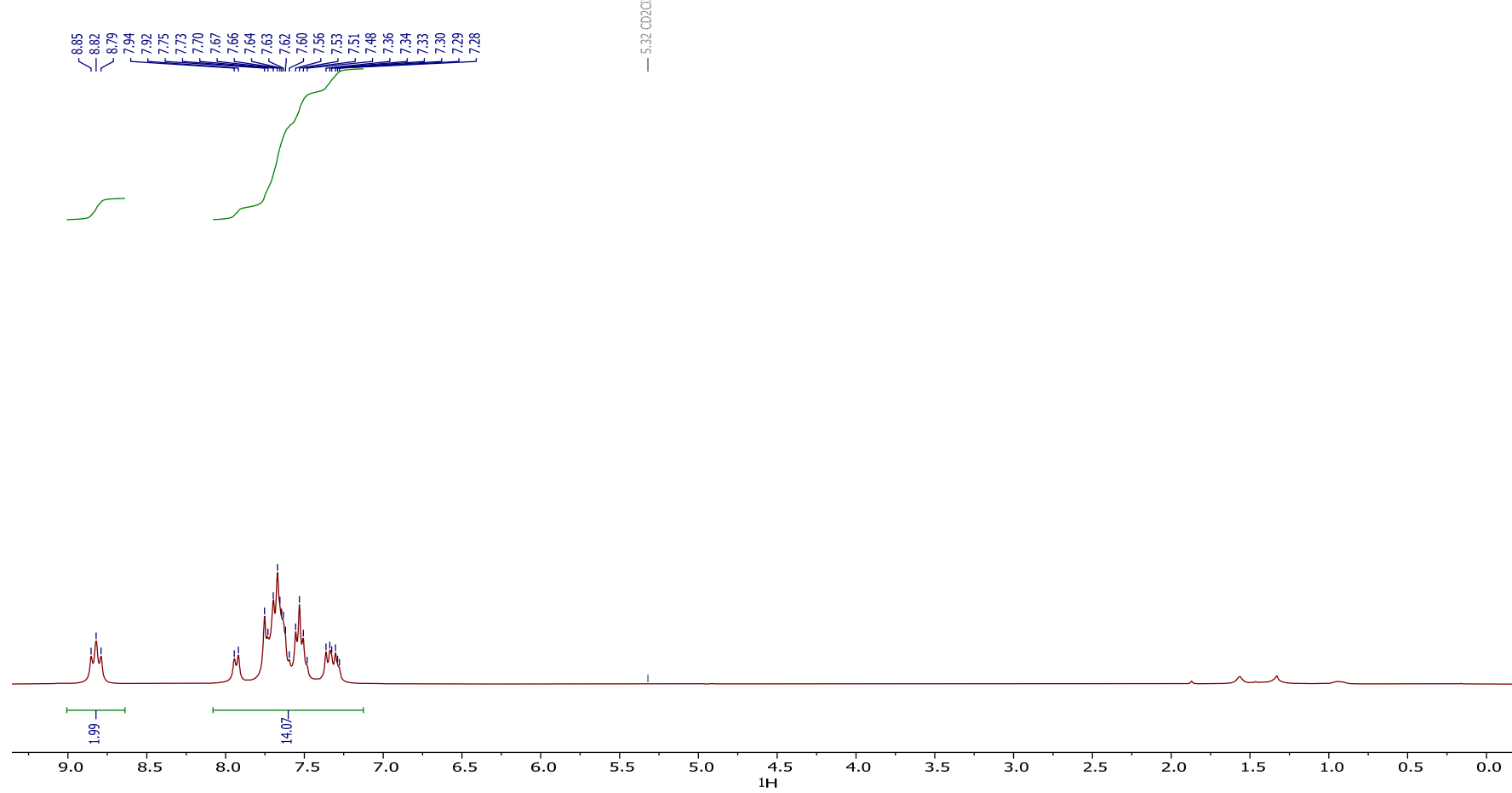


DEPT (CDCl_3)

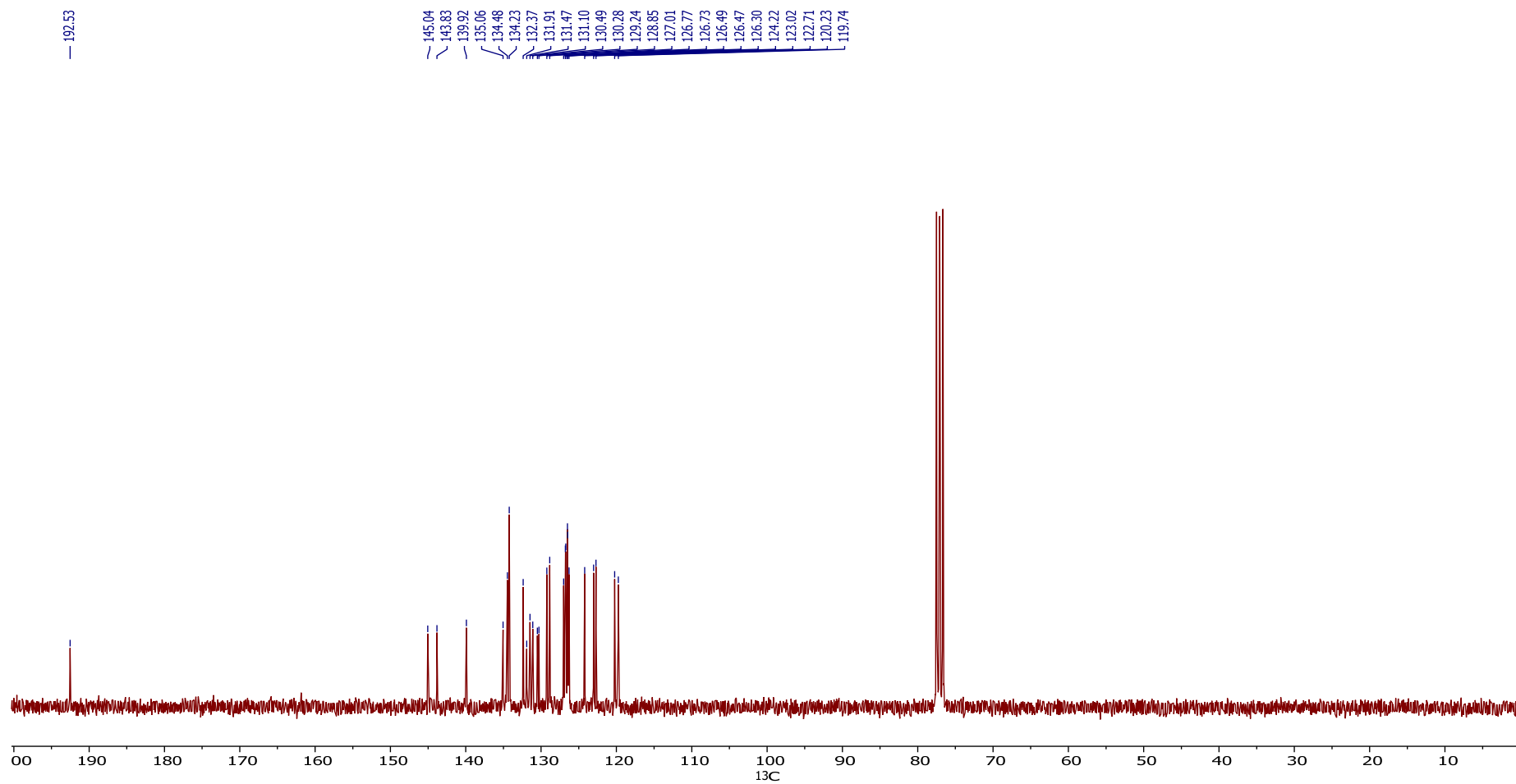


1-Phen-FO

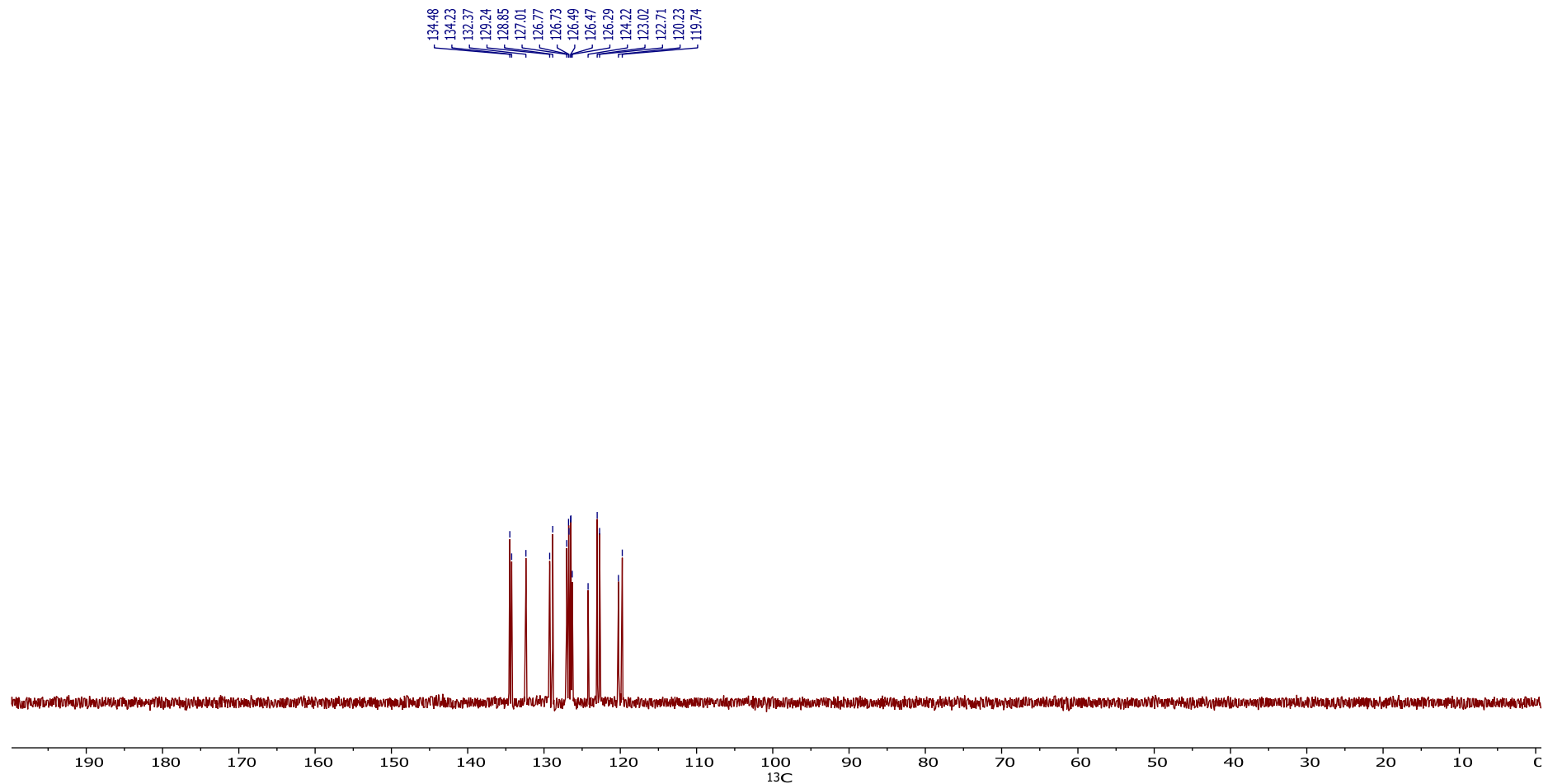
^1H (CD_2Cl_2)



¹³C (CDCl₃)

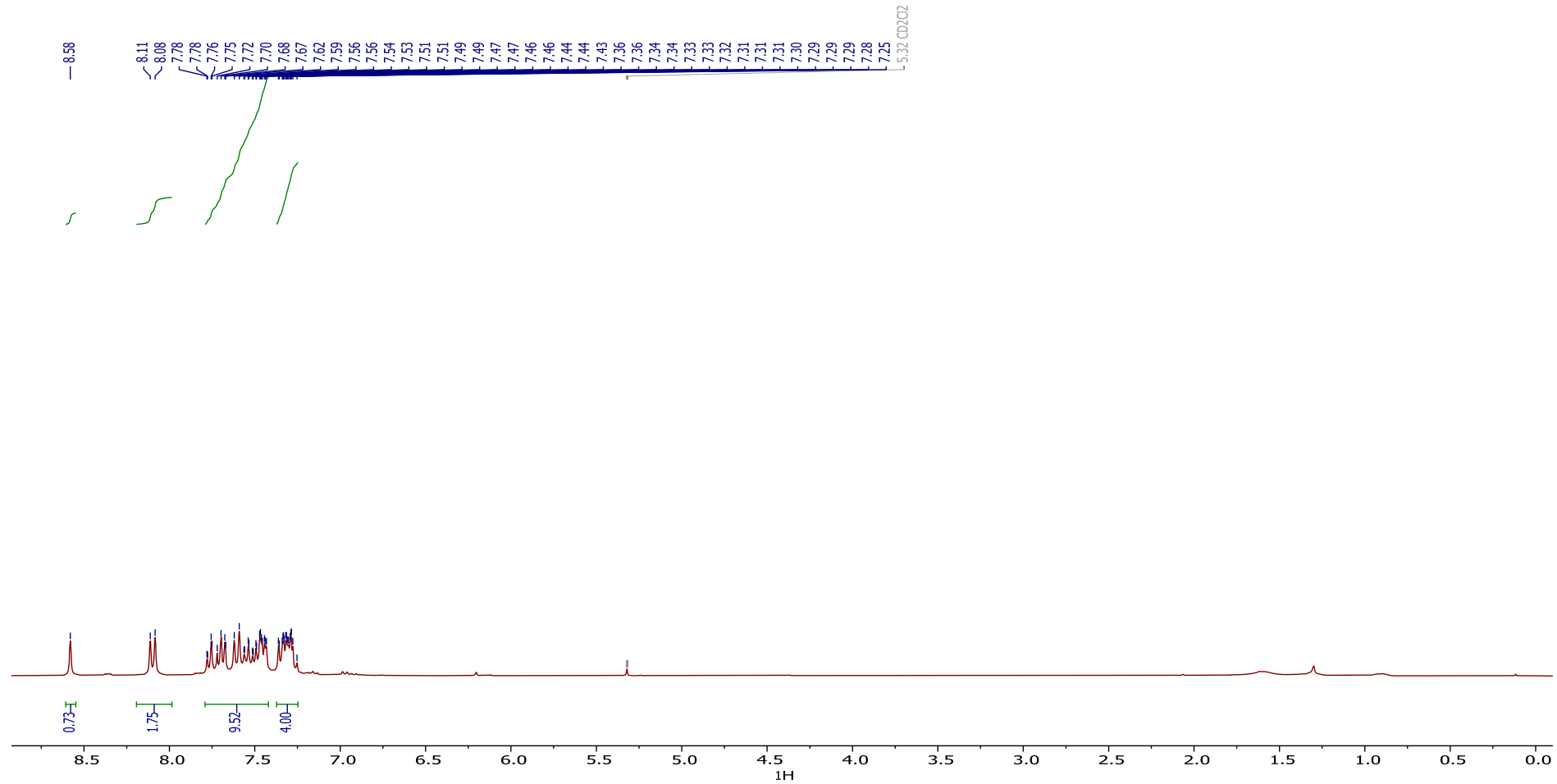


DEPT (CDCl_3)

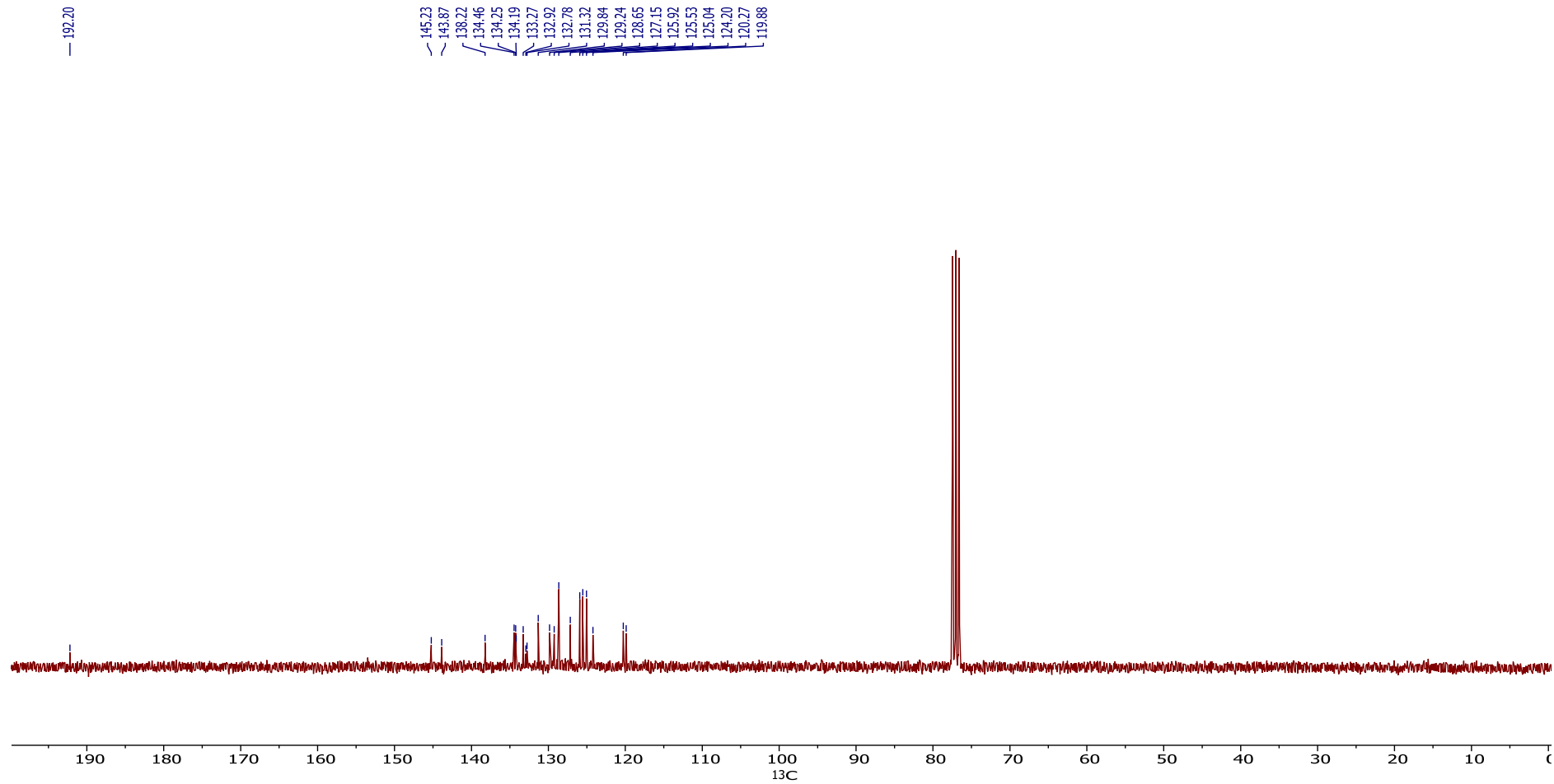


1-Anth-FO

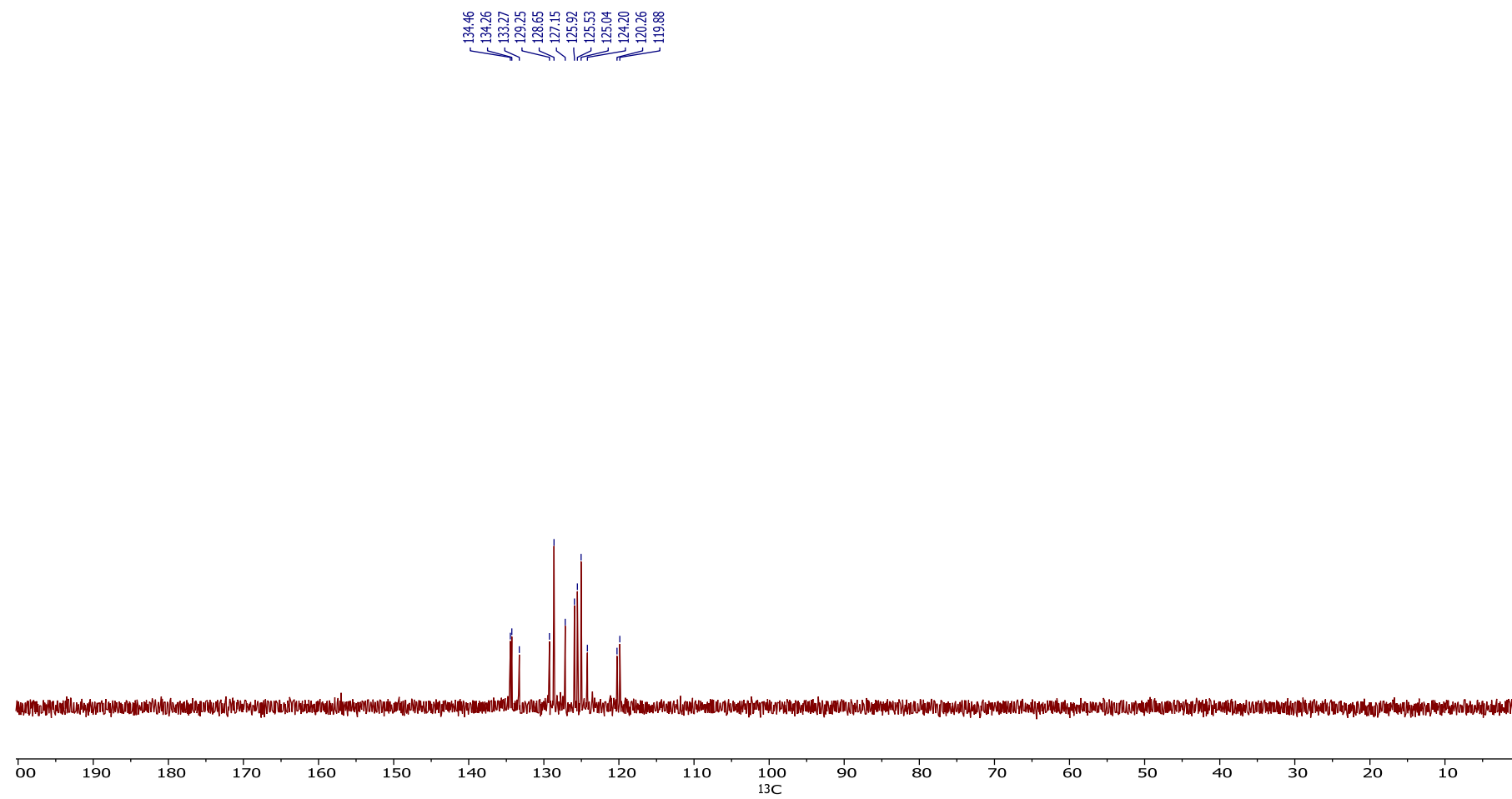
^1H (CD_2Cl_2)



¹³C (CDCl₃)

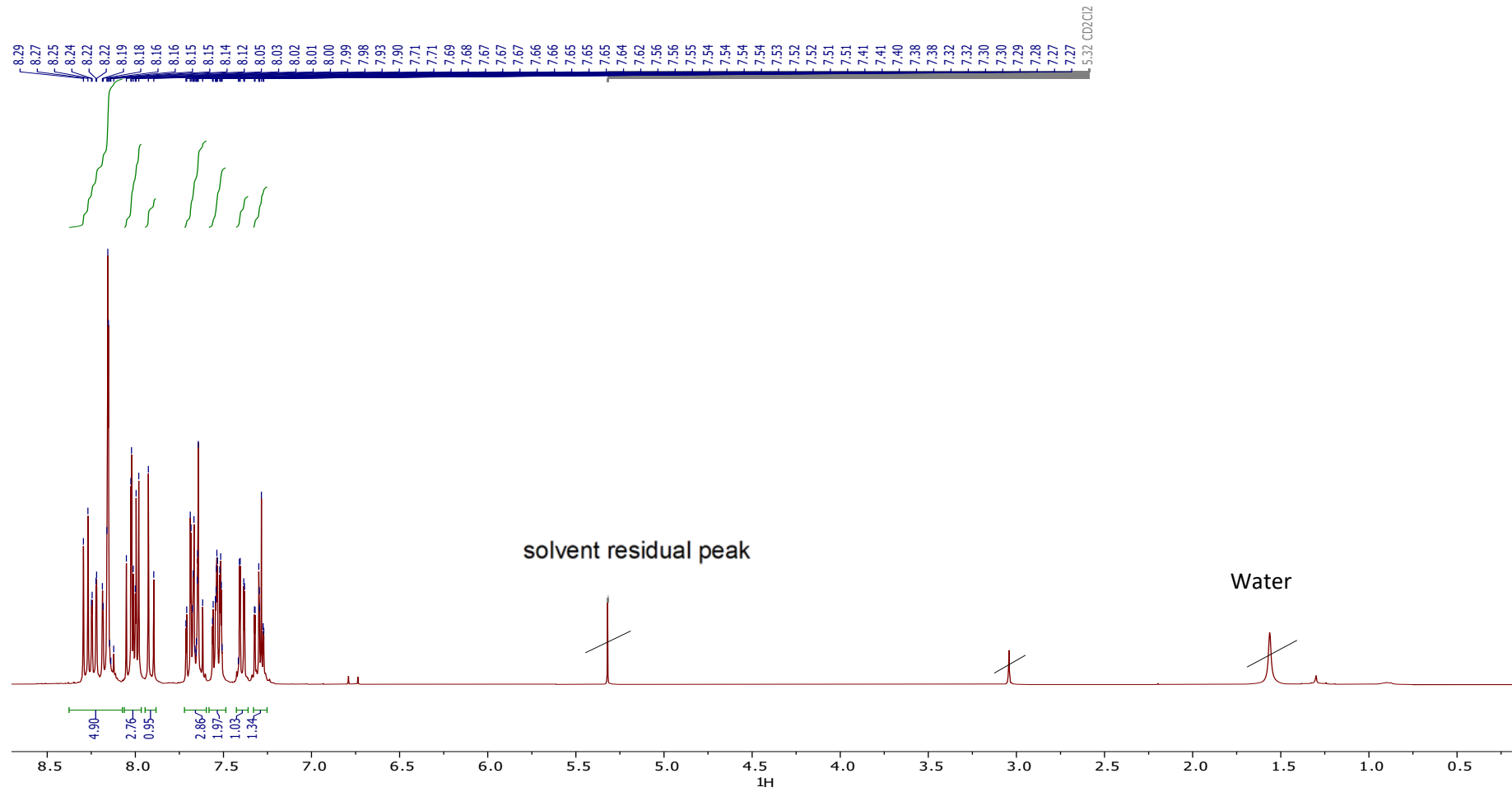


DEPT (CDCl_3)

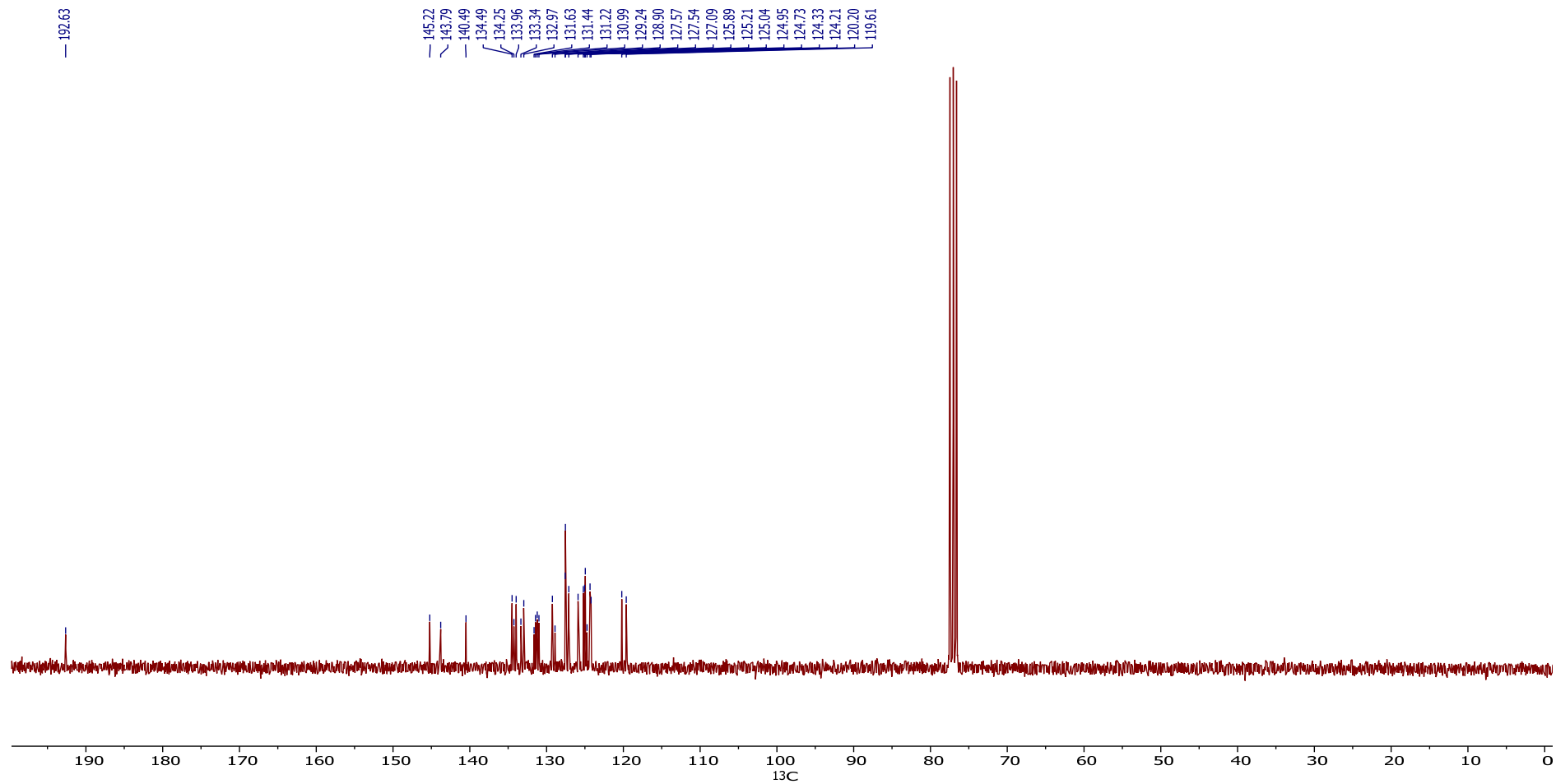


1-Pyr-FO

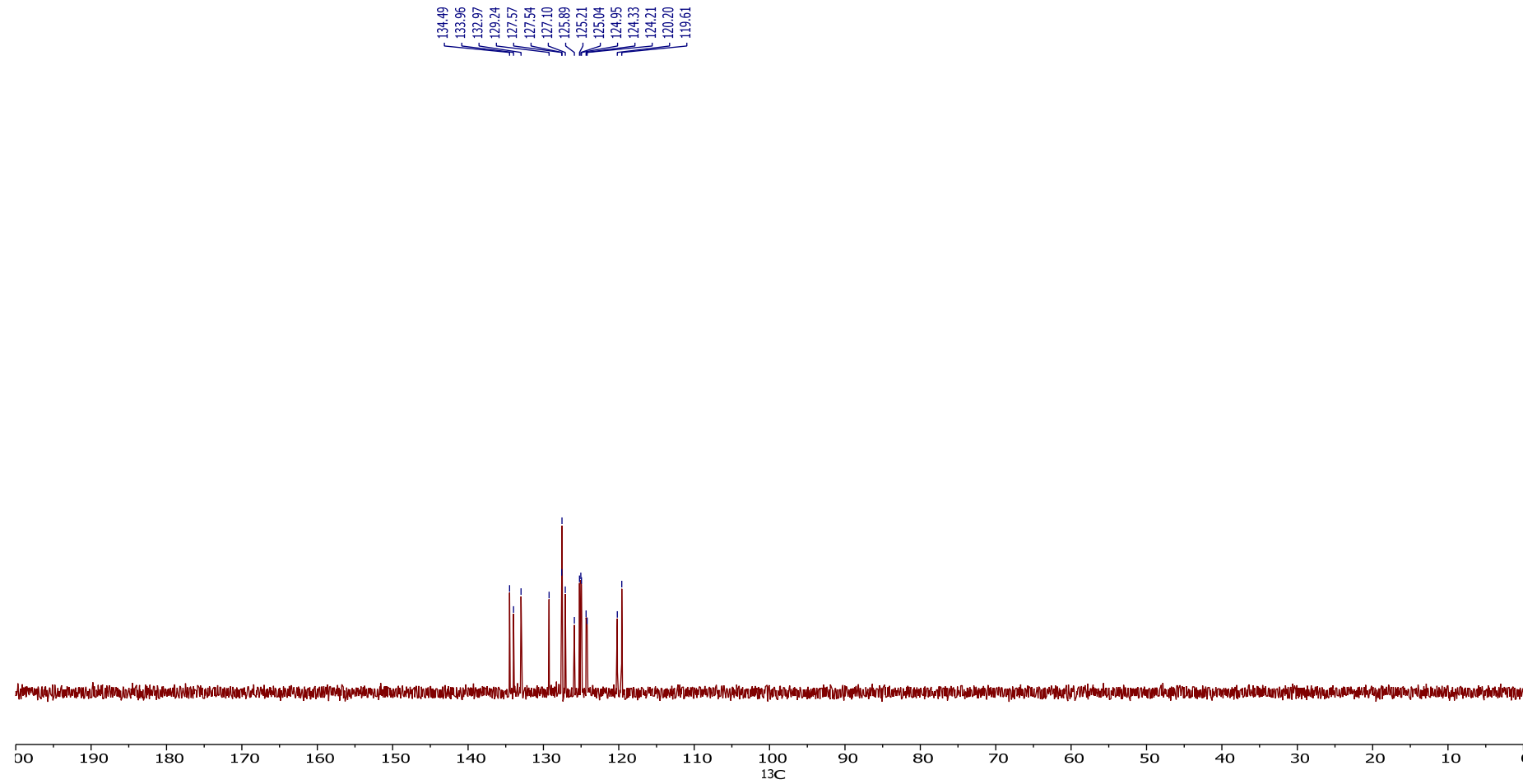
^1H (CD_2Cl_2)



^{13}C (CDCl_3)

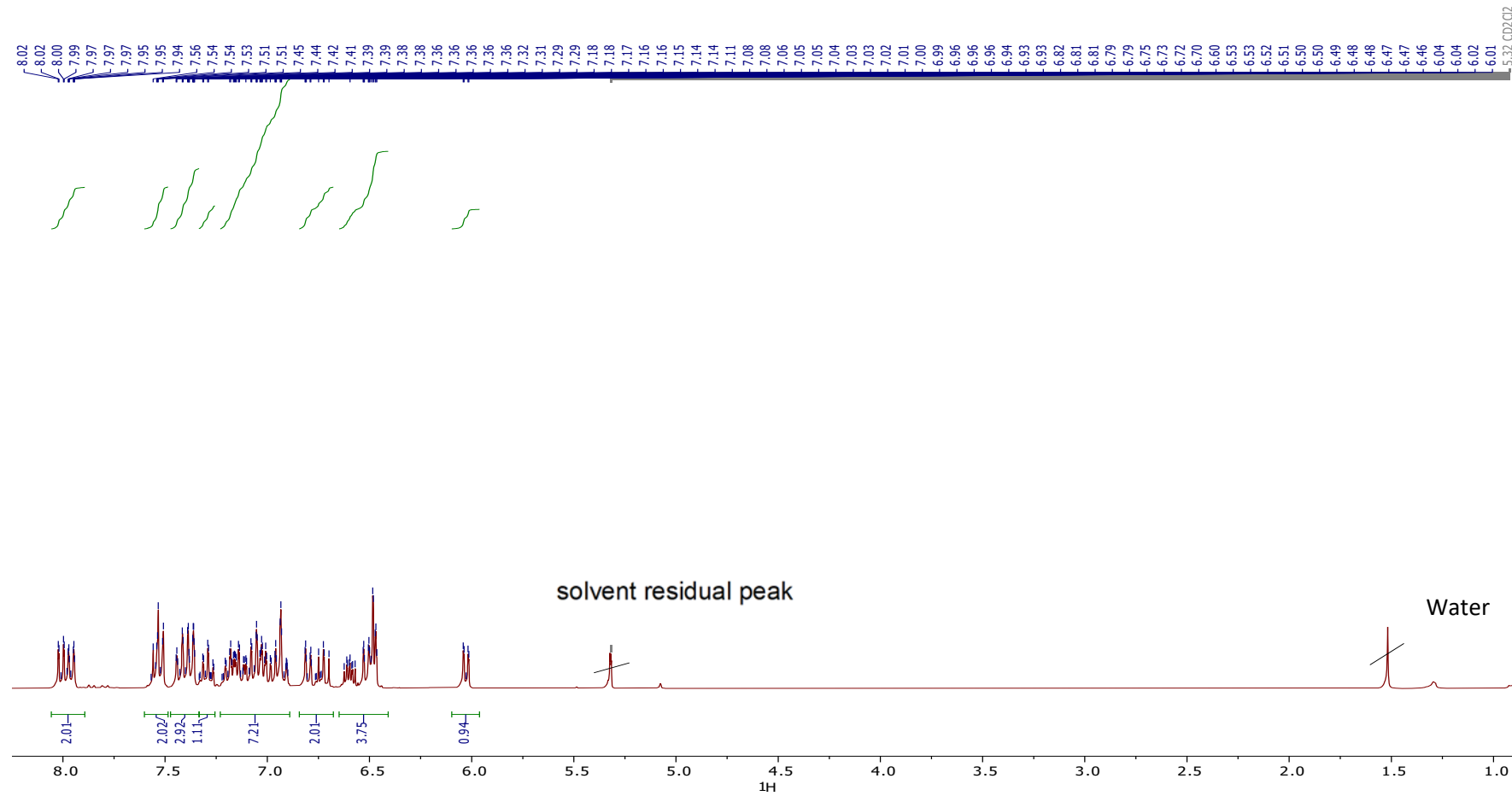


DEPT (CDCl_3)

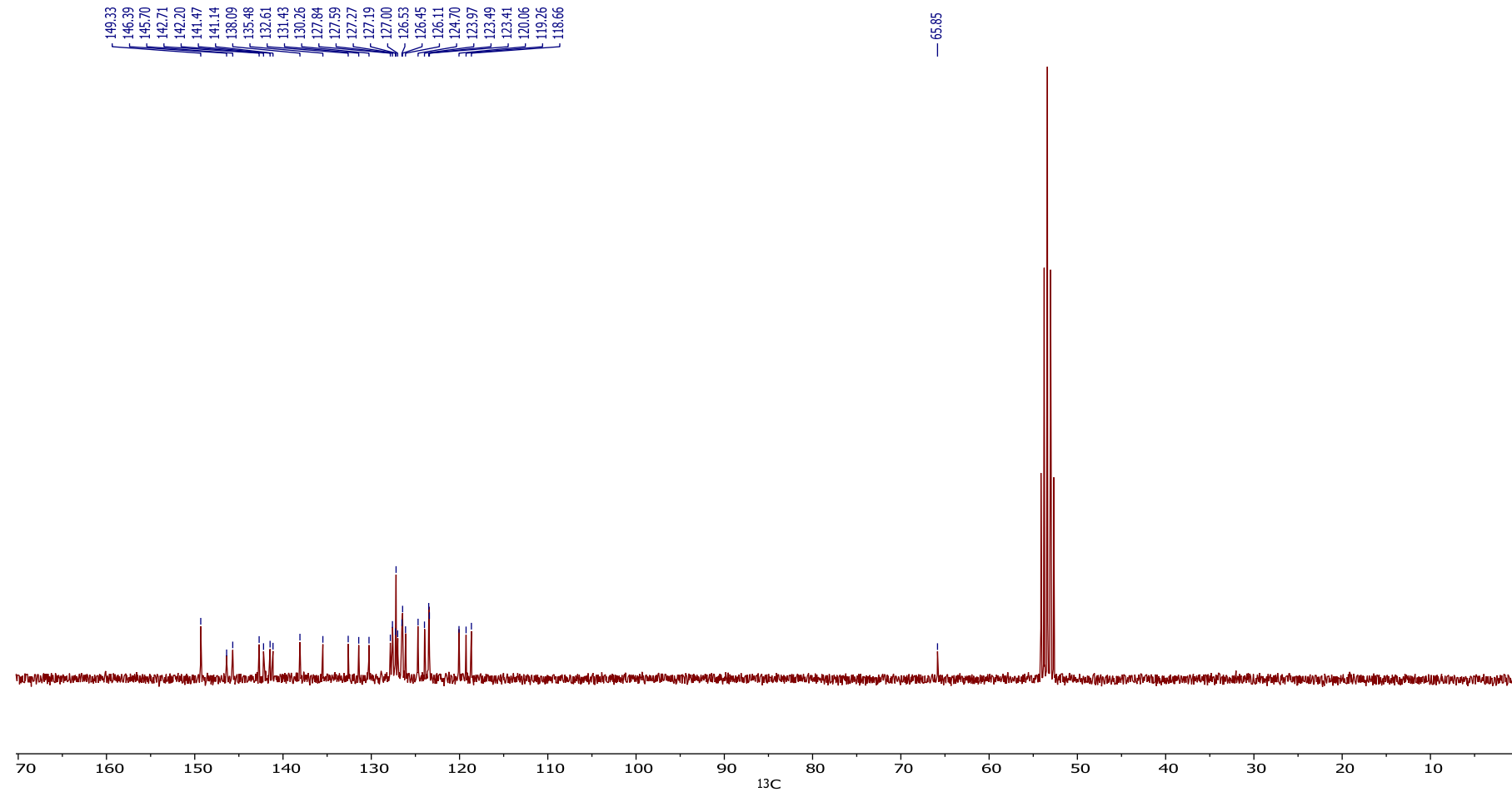


1-Napht-SBF

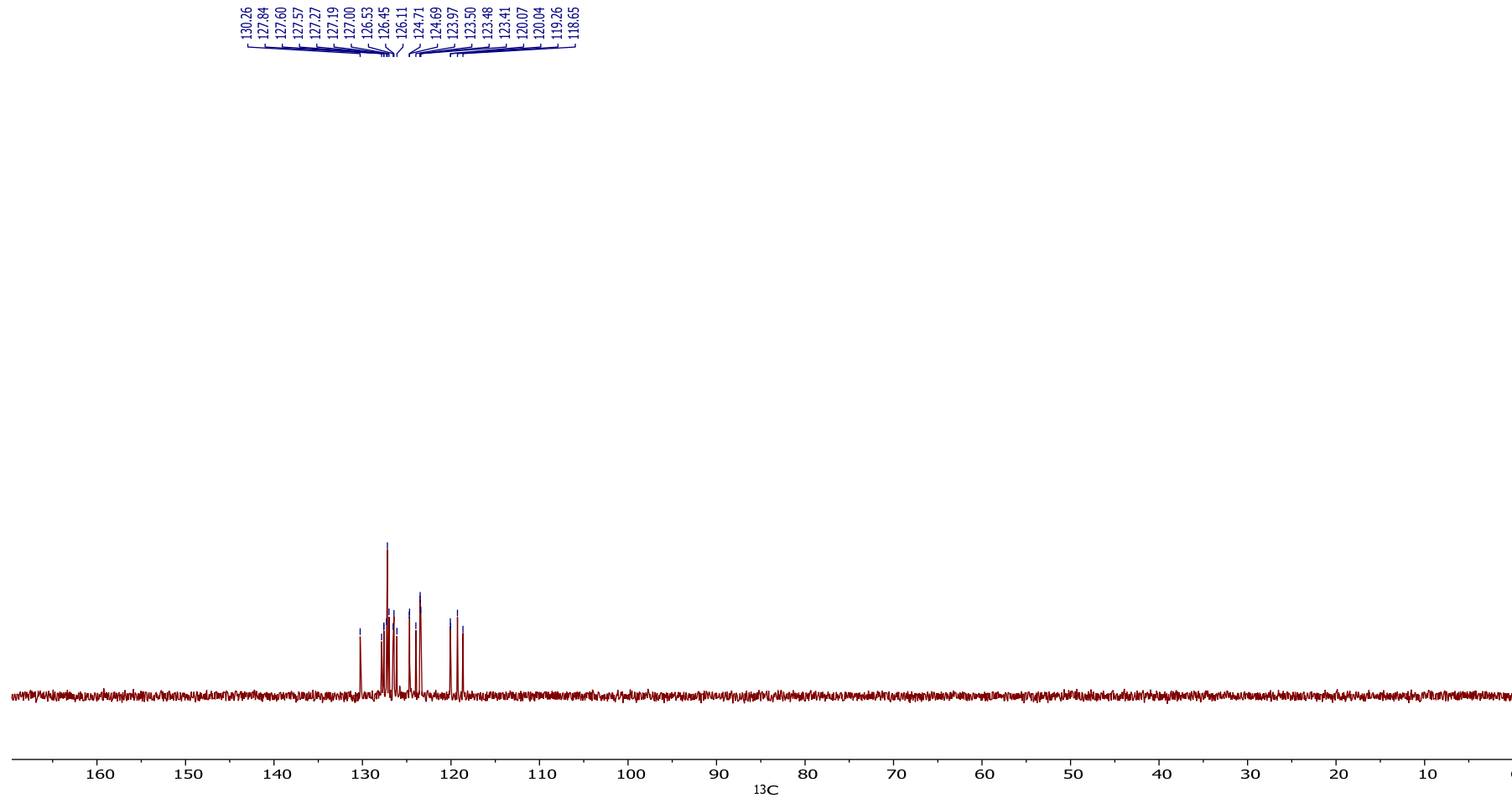
^1H (CD_2Cl_2)



^{13}C (CD_2Cl_2)

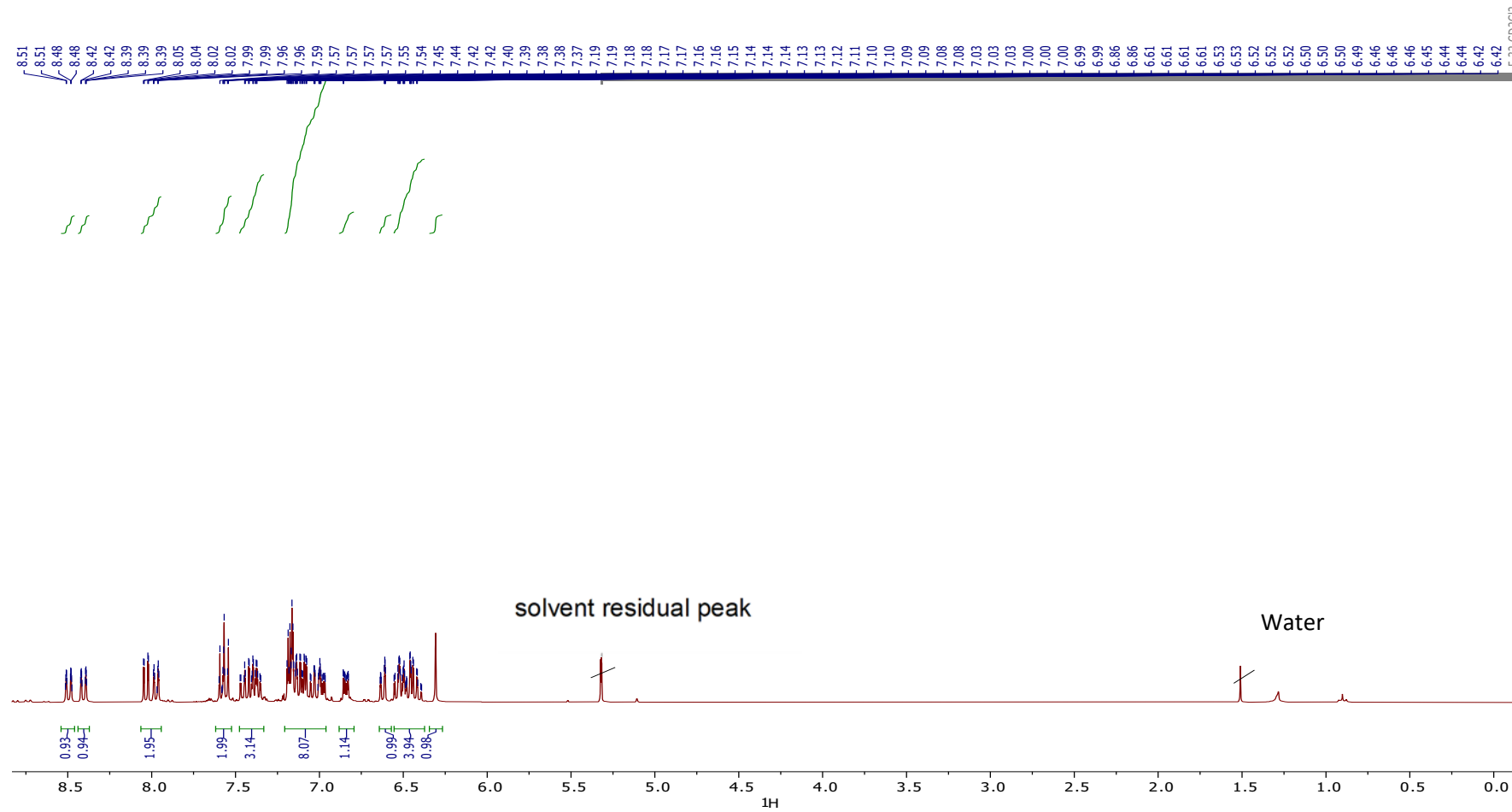


DEPT (CD_2Cl_2)

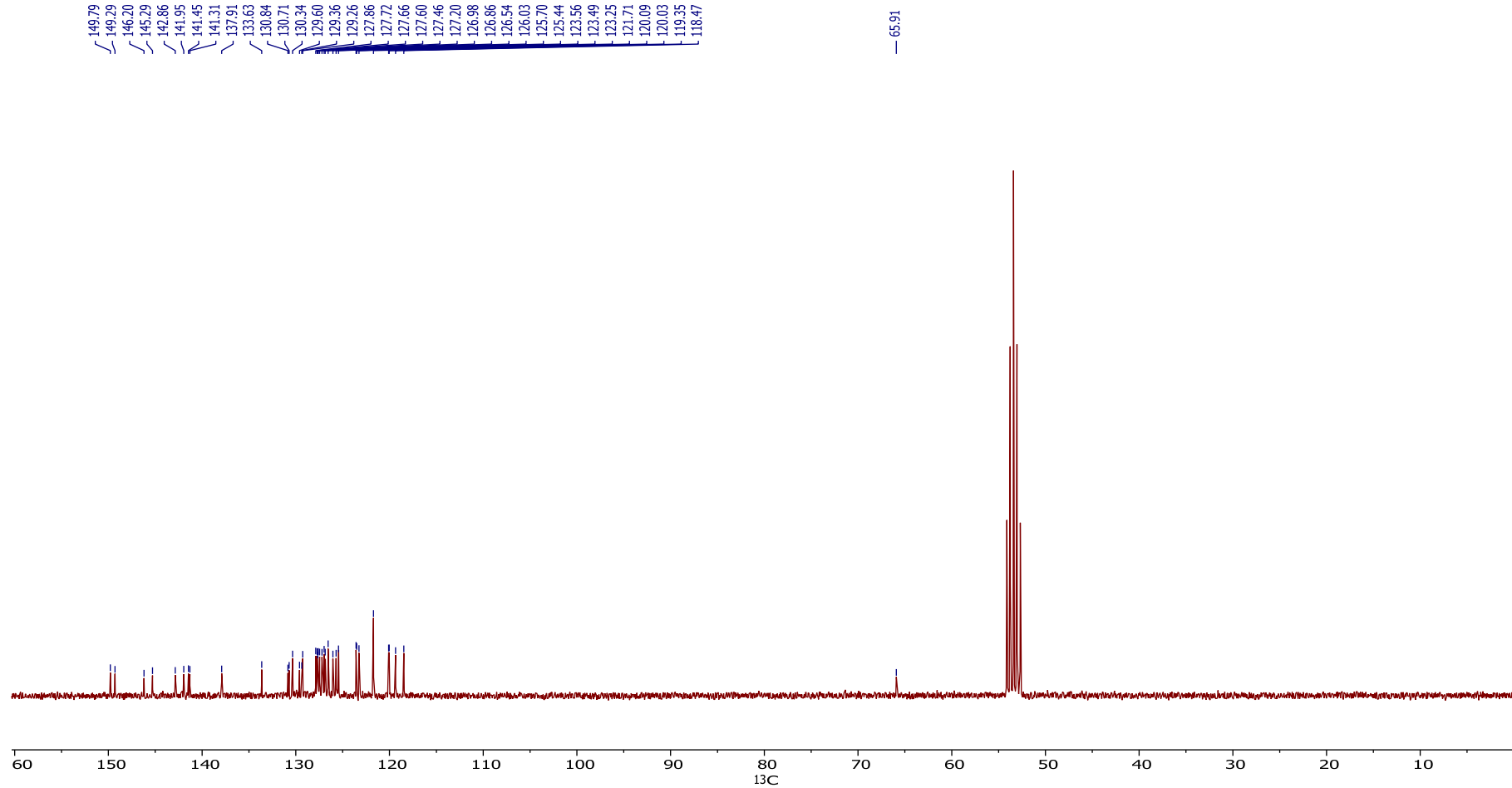


1-Phen-SBF

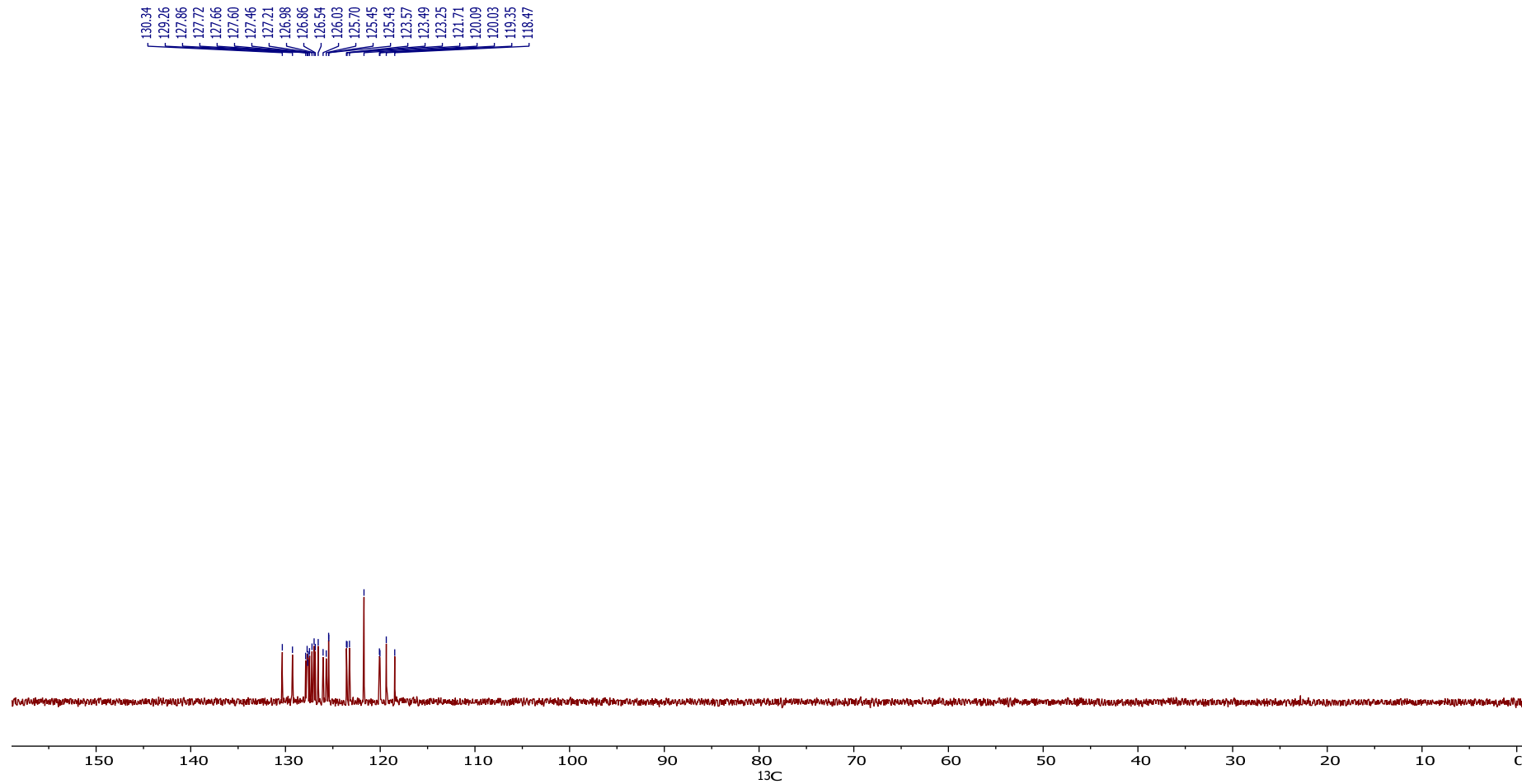
^1H (CD_2Cl_2)



¹³C (CD₂Cl₂)

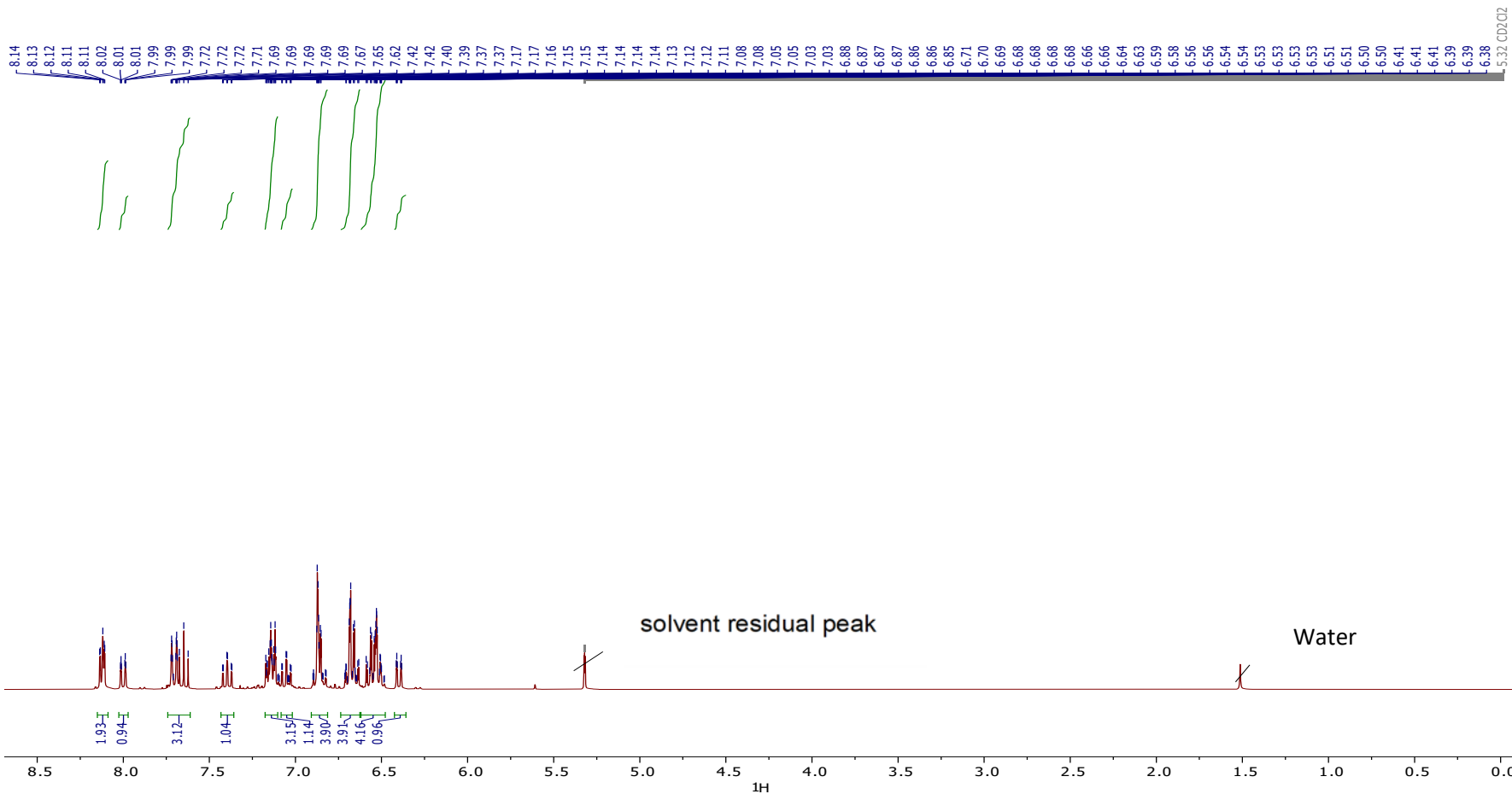


DEPT (CD₂Cl₂)

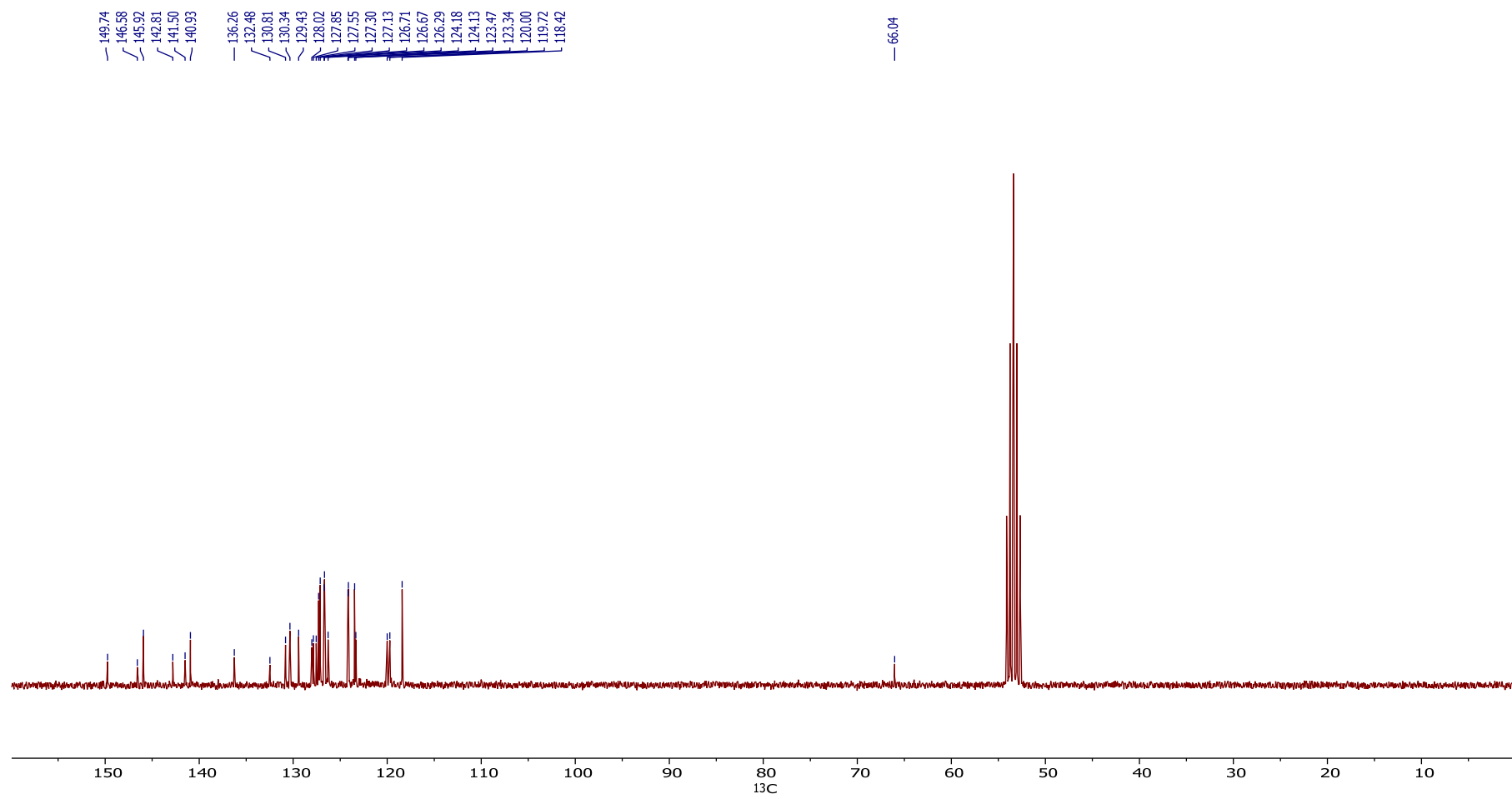


1-Anth-SBF

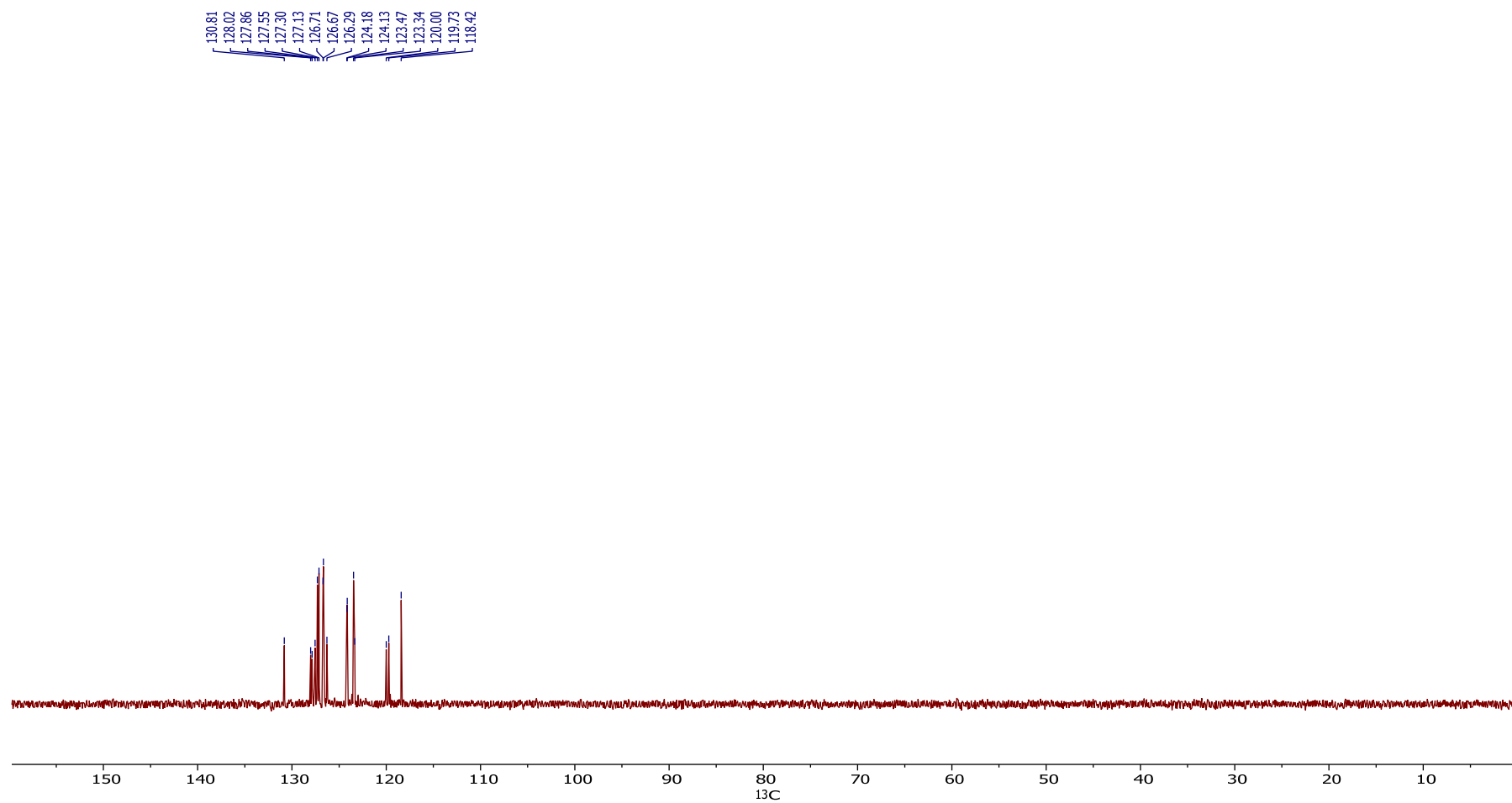
¹H (CD₂Cl₂)



¹³C (CD₂Cl₂)

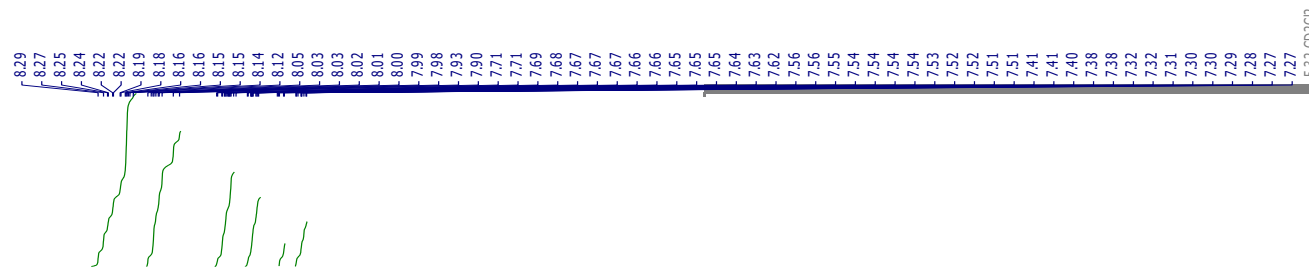


DEPT (CD_2Cl_2)



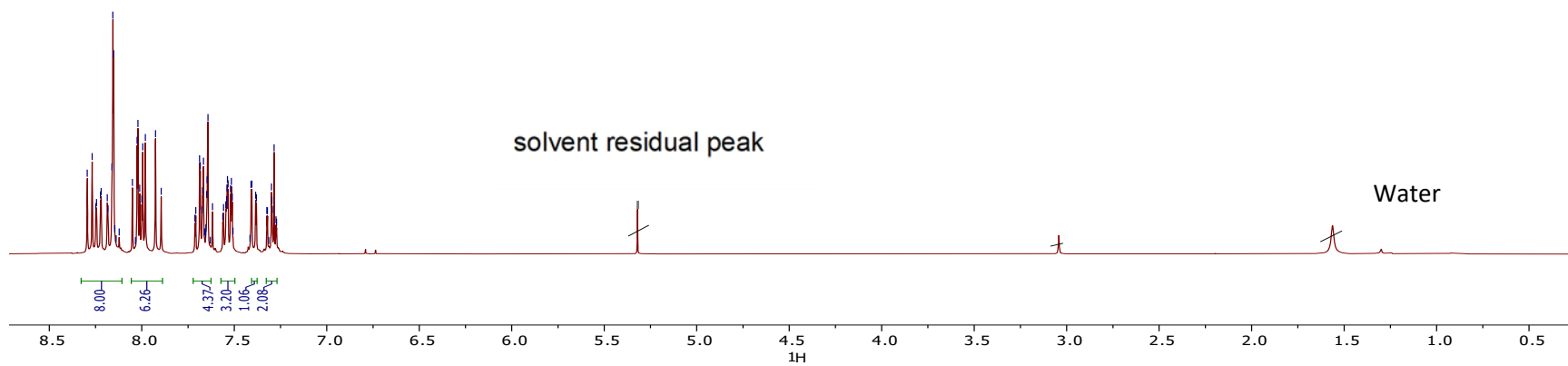
1-Pyr-SBF

^1H (CD_2Cl_2)

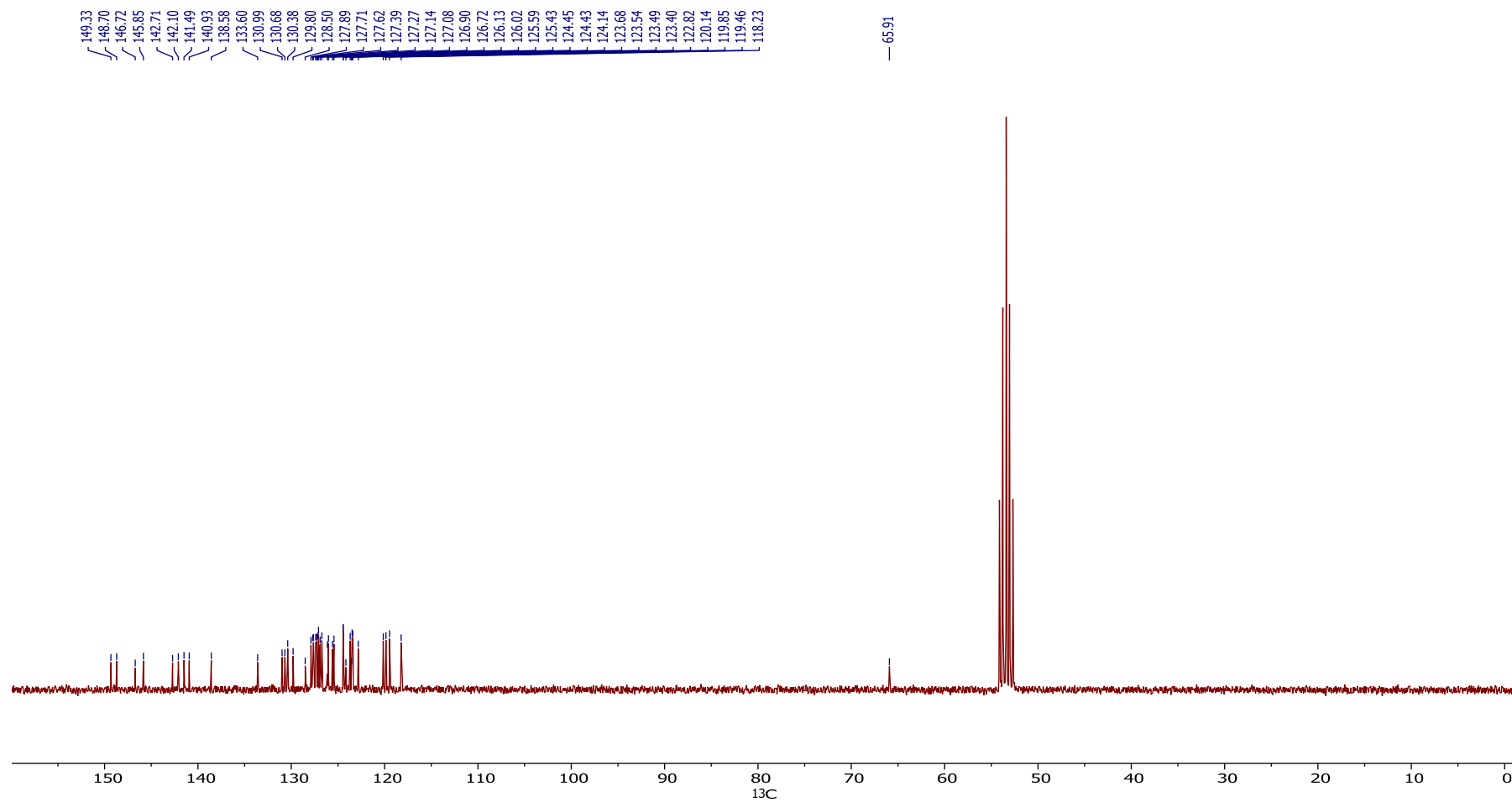


solvent residual peak

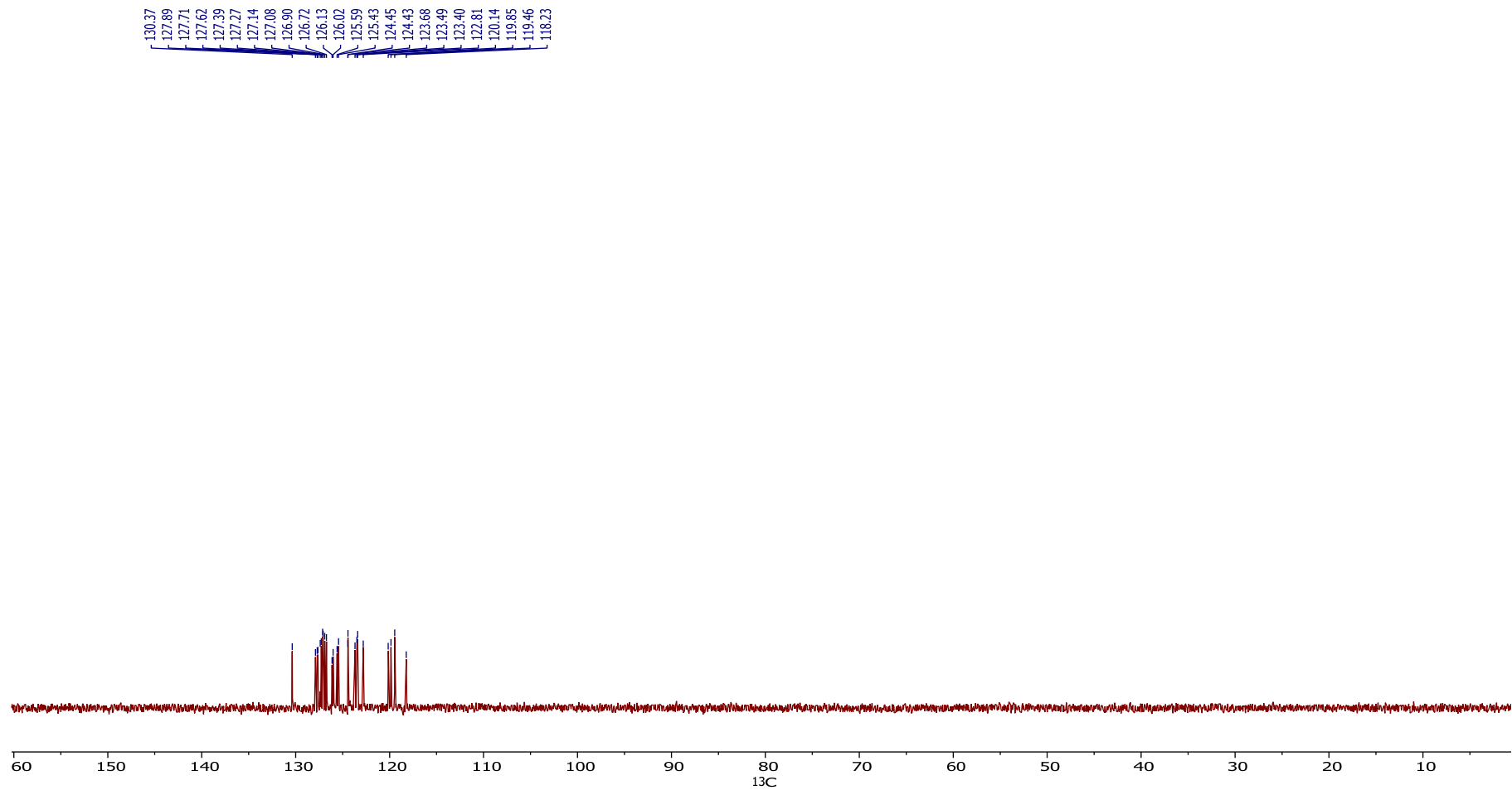
Water



^{13}C (CD_2Cl_2)



DEPT (CD_2Cl_2)



References

- 1.Fulmer, G. R.; Miller, A. J. M.; Sherden, N. H.; Gottlieb, H. E.; Nudelman, A.; Stoltz, B. M.; Bercaw, J. E.; Goldberg, K. I., *Organometallics* **2010**, 29, 2176.
- 2.Altomare, A.; Cascarano, G.; Giacovazzo, C.; Guagliardi, A.; Burla, M. C.; Polidori, G.; Camalli, M., *J. Appl. Cryst.* **1994**, 27, 435.
- 3.Sheldrick, G., *Acta Cryst. C* **2015**, 71, 3.
- 4.Farrugia, L., *J. Appl. Cryst.* **2012**, 45, 849.
- 5.Kulkarni, A. P.; Tonzola, C. J.; Babel, A.; Jenekhe, S. A., *Chem. Mater.* **2004**, 16, 4556.
- 6.Poriel, C.; Ferrand, Y.; Juillard, S.; Le Maux, P.; Simonneaux, G., *Tetrahedron* **2004**, 60, 145.
- 7.Sicard, L.; Quinton, C.; Lucas, F.; Jeannin, O.; Rault-Berthelot, J.; Poriel, C., *J. Phys. Chem. C* **2019**, 123, 19094.
- 8.Zhang, H.; Yu, T.; Zhao, Y.; Fan, D.; Xia, Y.; Zhang, P., *Synth. Met.* **2010**, 160, 1642.